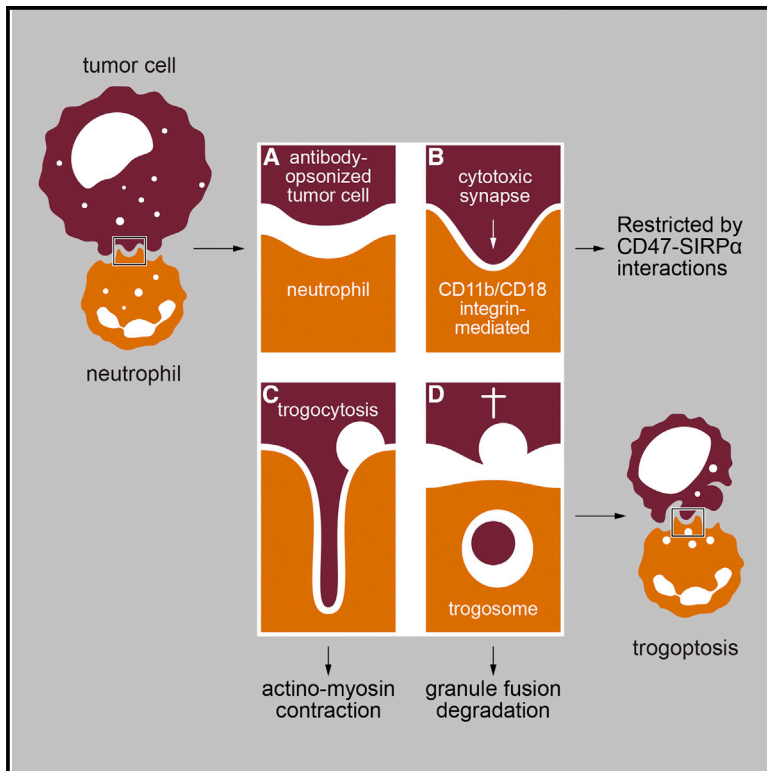


Neutrophils Kill Antibody-Opsonized Cancer Cells by Trogoptosis

Graphical Abstract



Authors

Hanke L. Matlung, Liane Babes, Xi Wen Zhao, ..., Taco W. Kuijpers, Paul Kubes, Timo K. van den Berg

Correspondence

t.k.vandenberg@sanquin.nl

In Brief

Matlung et al. identify trogoptosis as an immune cell-mediated mechanism of cytotoxicity, demonstrating that neutrophil-mediated destruction of antibody-opsonized cancer cells occurs through a specific process that is distinct from that used by other immune cells.

Highlights

- Neutrophils kill antibody-opsonized cancer cells by a process called trogoptosis
- Cancer cell plasma membrane ingestion by neutrophils is instrumental in trogoptosis
- Trogoptosis by neutrophils is further enhanced by CD47-SIRP α checkpoint inhibition



Neutrophils Kill Antibody-Opsonized Cancer Cells by Trogoptosis

Hanke L. Matlung,¹ Liane Babes,² Xi Wen Zhao,¹ Michel van Houdt,¹ Louise W. Treffers,¹ Dieke J. van Rees,¹ Katka Franke,¹ Karin Schornagel,¹ Paul Verkuijlen,¹ Hans Janssen,³ Pasi Halonen,⁴ Cor Lieftink,⁴ Roderick L. Beijersbergen,⁴ Jeanette H.W. Leusen,⁵ Jaap J. Boelens,^{6,7} Ingrid Kuhnle,⁸ Jutte van der Werff Ten Bosch,⁹ Karl Seeger,¹⁰ Sergio Rutella,¹¹ Daria Pagliara,¹² Takashi Matozaki,¹³ Eiji Suzuki,¹⁴ Catharina Willemien Menke-van der Houven van Oordt,¹⁵ Robin van Bruggen,¹ Dirk Roos,¹ Rene A.W. van Lier,¹ Taco W. Kuijpers,^{1,16} Paul Kubes,² and Timo K. van den Berg^{1,17,18,*}

¹Sanquin Research, and Landsteiner Laboratory, Academic Medical Center, University of Amsterdam, Amsterdam, the Netherlands

²Immunology Research Group, University of Calgary, Calgary, Alberta, Canada

³Division of Cell Biology, the Netherlands Cancer Institute, Amsterdam, the Netherlands

⁴Division of Molecular Carcinogenesis and the NKI Robotics and Screening Center, the Netherlands Cancer Institute, Amsterdam, the Netherlands

⁵Immunotherapy Laboratory, Laboratory for Translational Immunology, University Medical Center Utrecht, Utrecht, the Netherlands

⁶U-DANCE, Laboratory for Translational Immunology, UMC Utrecht, Utrecht, the Netherlands

⁷Department of Pediatrics, Blood and Marrow Transplantation Program, UMC Utrecht, Utrecht, the Netherlands

⁸Department of Pediatrics, University Medicine Göttingen, Göttingen, Germany

⁹Department of Pediatrics, Universitair Ziekenhuis Brussel, Brussels, Belgium

¹⁰Department of Pediatric Oncology/Hematology, Otto-Heubner-Center for Pediatric and Adolescent Medicine, Charité-Universitätsmedizin Berlin, Berlin, Germany

¹¹Division of Translational Medicine, Sidra Medical and Research Center, Doha, Qatar

¹²Department of Pediatric Hematology/Oncology, IRCCS Bambino Gesù Children's Hospital, Rome, Italy

¹³Department of Biochemistry and Molecular Biology, Division of Molecular and Cellular Signaling, Kobe University Graduate School of Medicine, Kobe 650-0017, Japan

¹⁴Department of Breast Surgery, Kyoto University Hospital, Kyoto, Japan

¹⁵Department of Medical Oncology, VU University Medical Center, Amsterdam, the Netherlands

¹⁶Emma Children's Hospital, Academic Medical Centre, University of Amsterdam, Amsterdam, the Netherlands

¹⁷Department of Molecular Cell Biology and Immunology, VU Medical Center, Amsterdam, the Netherlands

¹⁸Lead Contact

*Correspondence: t.k.vandenberg@sanquin.nl

<https://doi.org/10.1016/j.celrep.2018.05.082>

SUMMARY

Destruction of cancer cells by therapeutic antibodies occurs, at least in part, through antibody-dependent cellular cytotoxicity (ADCC), and this can be mediated by various Fc-receptor-expressing immune cells, including neutrophils. However, the mechanism(s) by which neutrophils kill antibody-opsonized cancer cells has not been established. Here, we demonstrate that neutrophils can exert a mode of destruction of cancer cells, which involves antibody-mediated trogocytosis by neutrophils. Intimately associated with this is an active mechanical disruption of the cancer cell plasma membrane, leading to a lytic (i.e., necrotic) type of cancer cell death. Furthermore, this mode of destruction of antibody-opsonized cancer cells by neutrophils is potentiated by CD47-SIRP α checkpoint blockade. Collectively, these findings show that neutrophil ADCC toward cancer cells occurs by a mechanism of cytotoxicity called trogoptosis, which can be further improved by targeting CD47-SIRP α interactions.

INTRODUCTION

Therapeutic monoclonal antibodies directed against tumor antigens expressed on cancer cells have been a valuable alternative or addition to conventional cancer treatment modalities such as chemotherapy for >25 years (Glennie and van de Winkel, 2003; Oldham and Dillman, 2008). In general, cancer therapeutic antibodies act by a combination of direct and indirect immune-mediated effects, including complement-dependent cytotoxicity and antibody-dependent cellular cytotoxicity (ADCC). ADCC can be mediated through the activation of different Fc receptors and by different Fc receptor-expressing cells, such as natural killer (NK) cells, macrophages, and neutrophils (Albanesi et al., 2013; Bryceson and Long, 2008; Musolino et al., 2008; Nimmerjahn and Ravetch, 2008; Strome et al., 2007). Whereas the different Fc γ receptors involved in inducing ADCC, Fc γ RI, Fc γ RII, and Fc γ RIII have different binding affinities for immunoglobulin G (IgG) and different cell-specific expression, for neutrophils we have found Fc γ IIa to be the predominant Fc receptor inducing ADCC in breast cancer cells (Treffers et al., 2018). Furthermore, it is known that NK cells and macrophages primarily cause ADCC by granule-dependent apoptotic (Bryceson and Long, 2008) and phagocytic (Chao et al., 2010a; Gül et al., 2014; Montalvao et al., 2013) mechanisms, respectively. However, the cytotoxic mechanism(s) by which neutrophils destroy



antibody-opsonized cancer cells have remained essentially unknown (Albanesi et al., 2013; van Egmond and Bakema, 2013). Neutrophils frequently are encountered in human cancers (Eru-slanov et al., 2014), and there is compelling evidence that they contribute substantially to antibody-mediated tumor cell destruction *in vivo* (Albanesi et al., 2013; Hernandez-Ilizaliturri et al., 2003; Ring et al., 2017; Siders et al., 2010; Zhu et al., 2015). Furthermore, insight into the mechanism of neutrophil ADCC may offer opportunities for further improvement in the efficacy of antibody therapy in cancer.

In spite of the beneficial effects documented for various therapeutic antibodies against different types of cancer, antibodies alone are not curative and therefore there is a pertinent need to improve their efficacy. By analogy to T cell immunity against cancer, which can be promoted by the inhibitors of immune checkpoints such as programmed cell death-1-programmed cell death ligand-1 (PD1-PDL1) interactions (Topalian et al., 2015), we and others have demonstrated that targeting interactions between the “don’t-eat-me” signal CD47 on cancer cells and the inhibitory immunoreceptor signal regulatory protein α (SIRP α) expressed on myeloid cells, including macrophages and neutrophils, potentiates antibody-dependent cancer cell destruction by those cells both *in vitro* and *in vivo* (Barclay and van den Berg, 2014; Chao et al., 2010a; Soto-Pantoja et al., 2012; Weiskopf et al., 2013; Zhao et al., 2011, 2012a, 2012b). Furthermore, CD47 frequently is overexpressed on cancer cells, and the clinical efficacy of antibody therapy against both hematological and solid cancers is inversely related to the expression levels of CD47 (Chao et al., 2010a; Majeti et al., 2009; Zhao et al., 2011). SIRP α is known to function as a typical inhibitory receptor that upon CD47 binding recruits and activates the protein tyrosine phosphatases Src homology region 2 domain-containing phosphatase-1 and -2 (SHP-1 and SHP-2) (Barclay and van den Berg, 2014), and blocking CD47-SIRP α interactions promotes the phagocytosis of opsonized tumor cells by macrophages (Chao et al., 2010a; Jaiswal et al., 2009; Majeti et al., 2009). Nevertheless, the mechanism(s) by which blockade of the CD47-SIRP α checkpoint enhances antibody-dependent cancer cell killing by neutrophils is not known, and this clearly requires insight into the cytotoxic mechanism by which neutrophils destroy antibody-opsonized cancer cells.

Our findings, presented here, suggest that neutrophils can kill antibody-opsonized cancer cells by a process that involves the active mechanic destruction of the target cell plasma membrane, leading to a form of immune cell-mediated necrotic type of cell death. This type of cytotoxicity appears intimately linked to a process of antibody-dependent trogocytosis, in which neutrophils endocytose, in both a cancer therapeutic antibody- and a cell-cell contact-dependent fashion, cytoplasmic fragments of the target cells. Trogocytosis was identified originally by Tabiasco et al. (2002) as an active mechanism of plasma membrane transfer among host (immune) cells. While the actual function(s) of the process have remained largely elusive (Joly and Hudrisier, 2003), evidence for the possible relevance of trogocytosis via immune cells has accumulated more recently. Notably, trogocytosis has been implicated as acting as a tolerogenic mechanism that mediates shaving of the target antigen CD20 from tumor cells in the context of ritux-

imab treatment of B cell malignancies, thereby preventing further susceptibility of the cancer cells toward anti-CD20 antibody-mediated destruction (Taylor and Lindorfer, 2015; Valgardsdottir et al., 2017). Trogocytosis by the parasite *Entamoeba histolytica* also has been proposed to inflict necrotic tissue damage to host cells during infection, which uses a trogocytosis-like process to inflict necrotic tissue damage to the host (Ralston et al., 2014). In line with the latter, there is evidence that trogocytosis occurs during macrophage-mediated ADCC toward trastuzumab-opsonized breast cancer cells (Velmurugan et al., 2016), but a direct causal relation between immune cell-mediated trogocytosis and tumor cell killing was not demonstrated in these studies.

Here, we report direct evidence that neutrophil ADCC involves a trogocytosis-related necrotic process of tumor cell death, referred to as trogoptosis. In particular, we show that neutrophil trogocytosis, which occurs both *in vitro* and *in vivo* and critically involves CD11b/CD18-dependent conjugate formation, coincides in a spatiotemporal fashion with the trogoptotic (i.e., lytic) death of antibody-opsonized solid cancer cells. Finally, inhibition of neutrophil trogocytosis prevents target cell trogoptosis, whereas promotion of trogocytosis by interference of CD47-SIRP α interactions enhances killing.

RESULTS

Killing of Antibody-Opsonized Cancer Cells by Neutrophils Requires CD11b/CD18 Integrin-Dependent Conjugate Formation

To provide more insight into the mechanism of neutrophil ADCC toward cancer cells, we investigated whether neutrophil ADCC required direct cell-cell interactions. Indeed, intimate effector-target interactions, reminiscent of killer synapses that are well established to be required for cytotoxicity by NK cells and cytotoxic T lymphocytes (CTLs) (Dustin and Long, 2010) but also have been reported for neutrophils (van Spriel et al., 2001, 2003), were demonstrated during neutrophil ADCC using trastuzumab-opsonized breast cancer cells (Figure 1A). The extent to which these conjugates occur was quantified by ImageStream flow cytometry (Figure 1B). Interference with CD47-SIRP α interactions by, for example, knock down of CD47 in breast cancer target cells, which was shown to potentiate neutrophil ADCC (Zhao et al., 2011), enhanced conjugate formation (Figure 1C), but the overall appearance of the resultant conjugate was not notably altered by CD47 knockdown (data not shown). Conjugate formation by neutrophils required Fc γ receptor (Fc γ R) occupation by antibody-opsonized tumor cells and CD11b/CD18 integrin-mediated adhesion, as shown by antibody-blocking experiments (Figure 1C). Prevention of conjugate formation by blocking Fc γ receptor (Figure S1A) and, in particular, Fc γ R1a (Treffers et al., 2018; Figure S1B) or CD11b/CD18 integrins (Figure 1D) but not that of other CD18 (β 2)- and CD29 (β 1)-integrins (Figures S1C and S1D), essentially abolished ADCC. These findings were consistent with previous observations (van Spriel et al., 2001) and corroborated by using neutrophils from a rare patient with leukocyte adhesion deficiency (LAD)-1 syndrome (van de Vijver et al., 2012), which lacks CD18 integrins because of a mutation in the *ITGB2* gene encoding this protein (Figures

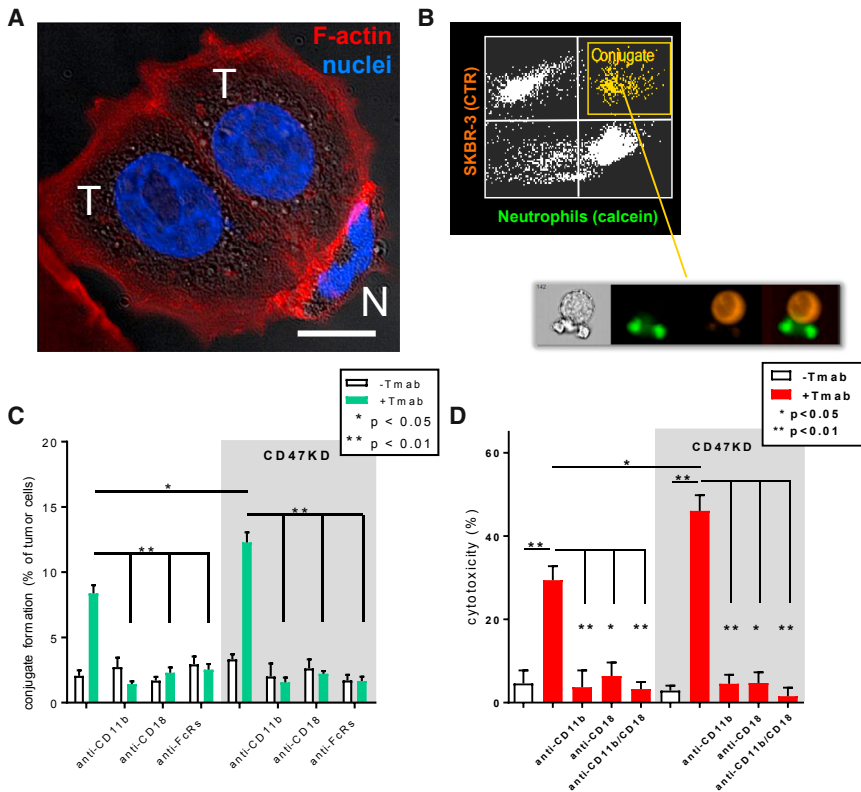


Figure 1. Neutrophil ADCC toward Cancer Cells Requires CD18 Integrin-Mediated Conjugate Formation

(A) Conjugate formation between a human neutrophil (N) and trastuzumab (Tmab)-opsonized SKBR3 breast cancer cells (T) as visualized by confocal fluorescence microscopy after staining of F-actin with phalloidin-rhodamine and nuclei with Hoechst. Note the accumulation of F-actin at the interface between the cells. Scale bar represents 10 μ m.

(B) ImageStream-X flow cytometric quantification of conjugate formation between calcein-AM-labeled (green fluorescence) neutrophils and Tmab-opsonized cell tracker red-labeled (red fluorescence) SKBR3 cells analyzed after 45 min incubation. A typical example of a microscopic image of a neutrophil-Tmab-cancer cell conjugate generated by the ImageStream-X flow cytometer also is shown.

(C) CD11b/CD18 and Fc γ receptor dependence of neutrophil conjugate formation with Tmab-opsonized SKBR3 cells, as shown by inhibition with anti-CD11b-blocking; anti-CD18-blocking antibodies; or a mixture of anti-CD64-, anti-CD32-, and anti-CD16-blocking antibodies (anti-FcRs). Data are average values \pm SEMs (n = 4 biological replicates, 2 independent experiments).

(D) Neutrophil ADCC requires conjugate formation as demonstrated by blocking with anti-CD11b, anti-CD18 antibodies, or both. Data are average values \pm SEMs (n = 3 biological replicates, 2 independent experiments). Statistical significance was tested with ANOVA followed by Sidak post-hoc test. *p \leq 0.05; **p \leq 0.01.

S1E–S1G). Thus, neutrophil cytotoxic conjugate formation is a strictly CD11b/CD18-dependent process, and it forms a prerequisite for ADCC toward cancer cells, both in the presence and absence of CD47-SIRP α interactions.

Antibody-Dependent Destruction of Cancer Cells by Neutrophils Involves a Non-apoptotic Mechanism Independent of Granule Exocytosis and the Phagocyte NADPH Oxidase

Because neutrophils lack the capacity to phagocytose cancer cells (Valgardsdottir et al., 2017), we evaluated whether human neutrophil ADCC was mediated by an extracellular mechanism dependent on granule exocytosis. For this purpose, we used neutrophils from rare familial hemophagocytic lymphohistiocytosis (FHL)-5 patients, which have mutations in the *STXBP2* gene encoding the munc18-2 protein (Figure S1E) (de Saint Basile et al., 2010; Meeths et al., 2010). Both neutrophils and NK cells from such patients have defects in granule release (Meeths et al., 2010; Zhao et al., 2013). Although evidence for granule exocytosis during ADCC was obtained by healthy control neutrophils, as exemplified by the release of myeloperoxidase (MPO) (Figure S2A), neutrophils of patients with FHL-5 showed completely normal killing of Her2/Neu⁺ breast cancer cells in the presence of the therapeutic anti-Her2/Neu monoclonal antibody trastuzumab (Tmab) (Figure S2B). In contrast, as expected, NK cell-mediated ADCC, which involves the release of granzymes and perforin from exocytosed granules that cause target

cell apoptosis (Bryceson and Long, 2008; Dustin and Long, 2010), was profoundly impaired (Figure S2C). These findings excluded a neutrophil extracellular granule-dependent mechanism of cytotoxicity during ADCC. Furthermore, the other major antimicrobial effector mechanism of neutrophils (Reeves et al., 2002; Segal, 2005), which involves the formation of reactive oxygen species by the phagocyte nicotinamide adenine dinucleotide phosphate (NADPH) oxidase, was also excluded by testing neutrophils from patients with chronic granulomatous disease (CGD) (Figures S1E, S2D, and S2E) having mutations in components of the NADPH oxidase, causing a complete lack of production of reactive oxygen species (Roos et al., 2003; Segal, 2005). Finally, the possible redundancy between both effector pathways could be excluded as well because inhibition of NADPH oxidase by diphenyleneiodonium (DPI) in neutrophils from patients with FHL-5 did not significantly affect their ADCC capacity (Figure S2F).

Neutrophil and NK cell-mediated ADCC appeared to involve different types of cell death, because neutrophil-mediated ADCC was not influenced by the use of the caspase inhibitor N-Benzyloxycarbonyl-Val-Ala-Asp(O-Me) fluoromethyl ketone (Z-VAD-FMK) (Figure S2G). In addition, neutrophils did not induce the typical signs of apoptotic cancer cell death, as is seen with NK cells as effector cells (Figure S2H). Rather, neutrophil-mediated ADCC seemed to involve a non-apoptotic type of cell death associated with cell lysis and loss of cytoplasmic material.

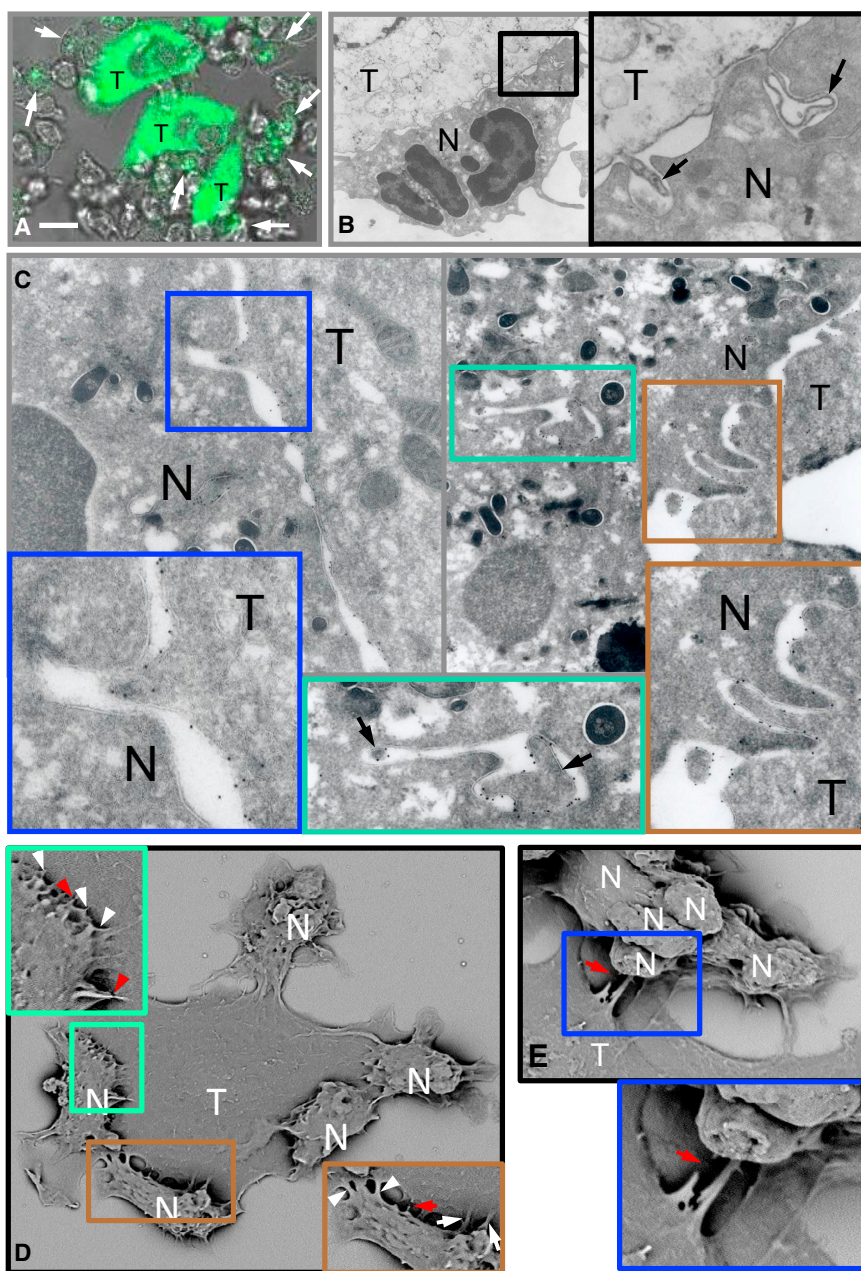


Figure 2. Neutrophils Cause Antibody-Opsonized Cancer Cell Destruction by Trogoptosis

(A) Antibody-dependent trogocytic uptake of cancer cell membrane material by human neutrophils. Neutrophils were incubated with DiO-labeled SKBR3 breast cancer cells (T) at an effector:target cell (E:T) ratio of 5:1 in the presence of Tmab, and acquisition of labeled cancer membrane material by neutrophils (white arrows) was visualized by confocal fluorescent microscopy. Scale bar represents 10 μ m.

(B) Ultrastructural localization of trogocytic invaginations (black arrows) at the neutrophil (N) conjugate with a Tmab-opsonized SKBR3 cell (T). (C) Trogocytic uptake visualized by electron microscopy at the interface between Tmab-opsonized biotin-labeled SKBR3 cells and neutrophils (N). Note the initial trogocytic invaginations (blue and brown insets) and endosome-like vesicles (green inset) containing biotin-labeled tumor material (T).

(D and E) SEM images of the trogocytic process of antibody-opsonized SKBR3 CD47KD cells (T) by neutrophils (N). White arrows show intact cell-cell contacts between neutrophils and SKBR3 cells (D); red arrows show disruption of the target cell membrane (D and E). Images were made after 45-min incubation of neutrophils with antibody-opsonized tumor cells.

brane by the neutrophils (Videos S1 and S2; Figure 2A) in a way that was reminiscent of trogocytosis. Our subsequent ultrastructural analysis of conjugates of biotin-labeled breast cancer cells revealed trogocytic invaginations and sometimes cup-like structures containing target cell plasma membrane at the neutrophil surface, as well as endosome-like vesicles within the cytosol (Figures 2B and 2C). Simultaneous labeling for granule markers such as MPO or lactoferrin (LF), derived from azurophilic and specific neutrophil granules, respectively (Borregaard et al., 2007), identified tumor plasma membrane material within double-labeled phagosomes; this is indicative of endocytic ingestion, phago-

Neutrophils Kill Antibody-Opsonized Cancer Cells by Trogoptosis

We further explored the possible nature of the cytotoxic effector mechanism during neutrophil ADCC by live cell imaging. This revealed the dynamic nature of neutrophils, which is characterized by active migratory behavior, and the transient formation of conjugates with the cancer cells in the presence of Tmab (data not shown). When the cancer cell membranes were labeled with a hydrophobic fluorescent dye, such as 3,3'-dioctadecyloxycarbocyanine perchlorate (DiO), we observed that these contacts actually led to the acquisition of fragments of target cell mem-

brane by the neutrophils (Videos S1 and S2; Figure 2A) in a way that was reminiscent of trogocytosis. Our subsequent ultrastructural analysis of conjugates of biotin-labeled breast cancer cells revealed trogocytic invaginations and sometimes cup-like structures containing target cell plasma membrane at the neutrophil surface, as well as endosome-like vesicles within the cytosol (Figures 2B and 2C). Simultaneous labeling for granule markers such as MPO or lactoferrin (LF), derived from azurophilic and specific neutrophil granules, respectively (Borregaard et al., 2007), identified tumor plasma membrane material within double-labeled phagosomes; this is indicative of endocytic ingestion, phago-

some-azurophilic and -specific granule fusion, and phagolysosomal degradation (Figures S3A and S3B). Using scanning electron microscopy (EM), neutrophils were shown to form intimate interactions with the antibody-opsonized tumor cells (Figures 2D and 2E). A significant number of these contacts showed a disrupted appearance, which is indicative of active disruption of the target cell plasma membrane by the neutrophils.

To investigate whether neutrophil trogocytosis has a direct causal relation to target cell death, we monitored cancer cell plasma membrane destruction simultaneously by using target cells loaded with the cytosolic dye calcein (Videos S2 and S3;

Figure 3A). Both live cell imaging and flow cytometry analysis revealed that at least a proportion of the neutrophil interactions that were associated with trogocytosis led to a significant reduction in cancer cell cytoplasmic labeling (Figures 3B and 3C). Furthermore, neutrophil trogocytosis, as quantified by flow cytometry, was a rapid process that could be detected within 15 min (Figure 3D), and its kinetics coincided well with cytotoxic trogoptosis, as monitored by the ^{51}Cr release assay (Figure 3E). This time course of neutrophil killing during ADCC, which rapidly peaked within 2–4 hr, also was different from that of NK cell ADCC (Figure S3C), which requires apoptosis induction. It should be emphasized that it is not so much the antibody-induced trogocytosis that appears specific to neutrophils, but rather their capacity to induce the killing of opsonized target cells by a trogocytosis-related process. For instance, NK cells also are capable of trogocytosis in an antibody-dependent fashion. However, whereas the cytotoxicity of NK cells from patients with FHL-5 is essentially defective (Figure S2C), their trogocytosis appears to be unaffected by FHL-5 mutation (Figure S3D). Together, these data further emphasize the fundamentally different nature of the cytotoxicity evoked by the two types of immune effector cells.

Using a plasma membrane-impermeable LIVE/DEAD indicator, either present in the extracellular medium during the experiment (Video S4; Figures 4A–4F) or used at the end of the assay period (Figures 4G and 4H), revealed that neutrophil trogocytic interactions were causing a lytic (i.e., necrotic) form of cell death of the antibody-opsonized cancer cells, which we have proposed to call trogoptosis. Like conjugate formation, neutrophil trogocytosis and the associated trogoptosis were entirely antibody dependent (Figure 4H). Furthermore, as expected, neutrophil trogocytosis required conjugate formation, because it could be prevented by blocking CD11b/CD18 (Figure S3E). Neutrophil trogoptosis led to a significant and substantial loss of the plasma cell membrane of antibody-opsonized cancer cells, as determined by the reduction in Her2/neu expression (Figures 4I and 4J). Finally, quantification of the amount of 1,1'-Dioctadecyl-3,3,3',3'-Tetramethylindodicarbocyanine, 4-Chlorobenzenesulfonate Salt (DiD) staining shows that cancer cells that died from neutrophil interactions had lost more plasma cell membrane compared to cells that were still alive, further strengthening our conclusion that neutrophil trogocytosis is related causally to cell death of antibody-opsonized cancer cells (Figures 4K and 4L).

Our findings have consistently demonstrated that interference with CD47-SIRP α interactions, either by knocking down CD47 on cancer cells (Zhao et al., 2011 and data herein) or adding antagonistic antibodies against CD47 or SIRP α that had been shown to promote ADCC (Zhao et al., 2011) (Figure S4A), potentiated the effects of cancer therapeutic antibodies to trigger trogocytosis and killing. Neutrophil trogocytosis and the related cytotoxicity also were observed with other solid cancer target cell and therapeutic antibody combinations, as shown for A431 carcinoma cells. A431 carcinoma cells endogenously express the epidermal growth factor receptor (EGFR) in conjunction with the anti-EGFR antibody therapeutic cetuximab (Cmab) or by using A431 cells ectopically expressing the Her2 surface antigen in combination with Tmab (Figures S4C–S4F).

Trogocytosis and Trogoptosis by Neutrophils *In Vivo*

We investigated the possibility of the *in vivo* occurrence of neutrophil trogoptosis toward antibody-opsonized cancer cells in the Kupffer cell-depleted mouse liver using a B16F10 melanoma model (Gül et al., 2014). When CD47-SIRP α interactions were disturbed by SSL6, a *Staphylococcus aureus*-derived protein that binds to CD47 and is known to block CD47 binding to SIRP α (Fevre et al., 2014), the metastatic load of the tumor cells in the liver was strongly inhibited, demonstrating that interference of CD47-SIRP α interactions potentiates antibody-dependent tumor cell clearance by the remaining myeloid cells in this model (Figure 5A). This is consistent with enhanced mouse neutrophil-mediated destruction of the antibody-opsonized cancer cells observed *in vitro* (Figures S5A and S5B). Direct evidence for the prominent role of neutrophils as effector cells in this particular *in vivo* model was further obtained by the depletion of neutrophils by injection of the anti-Ly6G antibody (clone 1A8), which resulted in a significantly enhanced tumor load (Figure 5D). Using intravital microscopy, a significant amount of migratory neutrophils carrying tumor membrane material were seen in TA99-treated mice compared to isotype control treated animals (Figures 5B and 5C; Video S5). Furthermore, neutrophils could be observed that were actively involved in trogocytosing pieces of membrane from the antibody-opsonized tumor cells (Figure 5E; Video S6). Following propidium iodide injection, neutrophil-mediated trogoptotic cell death also could be demonstrated under these conditions (Figure 5F; Video S7).

Finally, immunohistochemistry or flow cytometry evaluation of the biopsies from patients with Her2-positive breast cancer that was responsive to neoadjuvant Tmab therapy revealed numerous neutrophils that had infiltrated the cancer tissue. Many of these neutrophils directly interacted with the breast cancer tissue and some had apparently taken up the Her2-containing cancer cell membrane, which is consistent with neutrophil trogocytosis of antibody-opsonized cancer cells in such patients (Figures S5C and 6A). Moreover, isolation of neutrophils from breast cancer tissue after Tmab treatment confirmed the intracellular staining for Her2 in neutrophils (Figures S5D and 6B). Collectively, the findings described above show that it is reasonable to assume that neutrophil trogocytosis and trogoptosis occur *in vivo* toward antibody-opsonized cancer cells in both mice and humans.

Intracellular Signaling in Neutrophils during Trogoptosis

To provide evidence that the induction of cancer cell trogoptosis by neutrophils is an active process that requires signaling downstream of Fc γ receptors in neutrophils, we tested the effect of pharmacological inhibition of the tyrosine kinase Syk, which is known to play a pivotal role upstream in the Fc γ receptor signaling cascade (Mócsai et al., 2010). Syk inhibition essentially abolished all aspects of the process, including conjugate formation, trogocytosis, and cytotoxicity (Figures 7A–7C), demonstrating that all of these responses require Fc γ receptor signaling in neutrophils. Further insight into the downstream signaling pathway(s) instrumental in neutrophil trogocytosis was obtained by performing an unbiased screen of 1,280 pharmacologically active compounds using our flow cytometric trogocytosis assay (Table S1). Among the selected compounds, we found inhibition

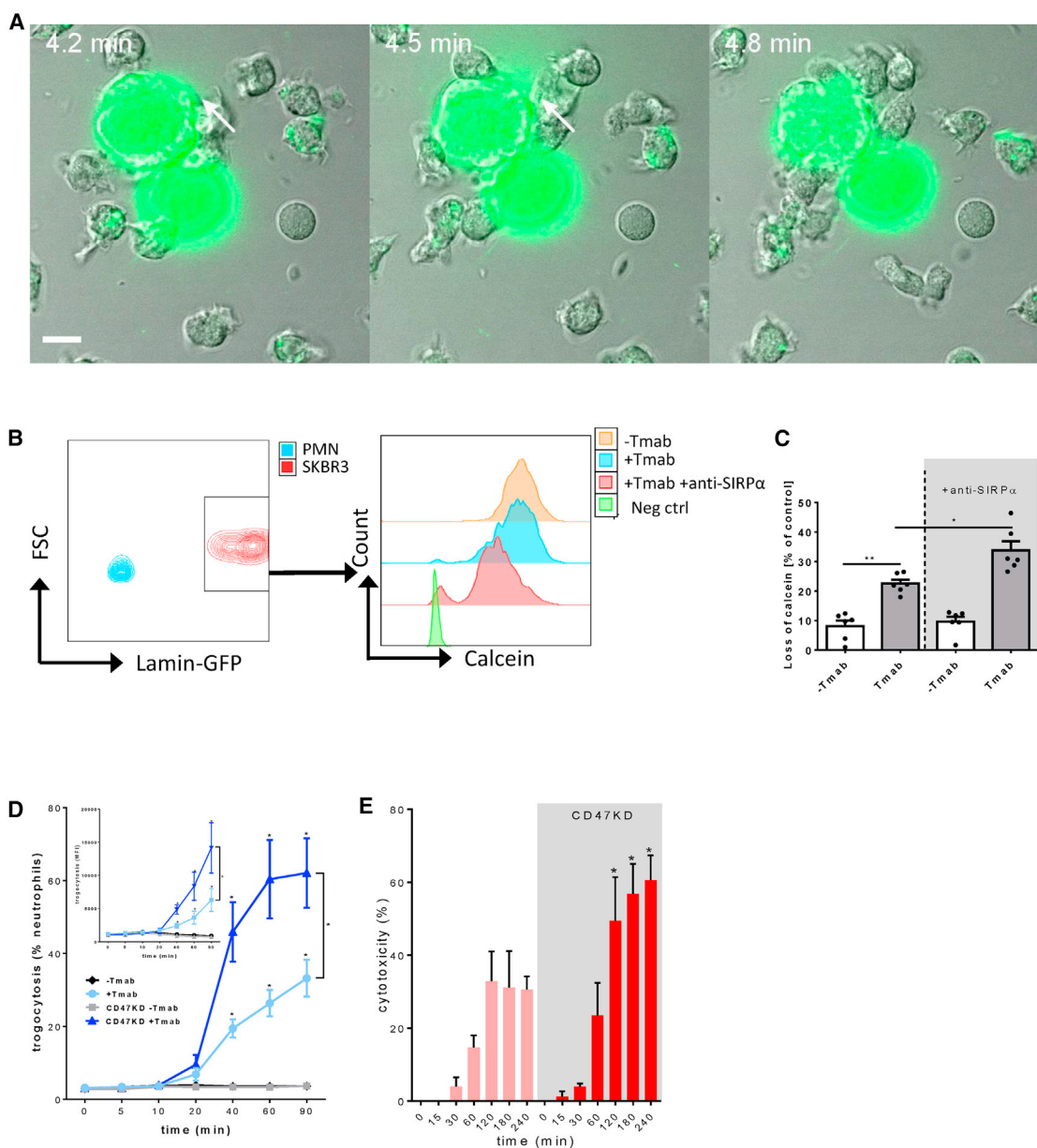


Figure 3. Trogocytosis of Antibody-Opsonized Cancer Cells by Neutrophils Leads to a Reduction in Cancer Cell Cytoplasmic Labeling and Coincides with Cytotoxicity

(A) Stills of the trogocytotic disruption (arrow) of a calcein-AM-labeled tumor cell (T) as revealed by live cell confocal video microscopy. Time (min) is indicated (upper left corner) from the start of the recording ~15 min after the initiation of the experiment, with the 3 frames covering a total period of 36 s extracted from Video S3. Scale bar represents 10 μ m.

(B) Gating strategy for fluorescence-activated cell sorting (FACS)-based trogocytosis and ADCC assay. SKBR3 cells are gated on the genetic expression of lamin B-GFP; neutrophils are negative for lamin B-GFP (left). SKBR3 cells lost the intracellular calcein red-orange label when opsonized with trastuzumab and incubated with neutrophils for 4 hr, and this calcein red-orange loss is enhanced when CD47-SIRP α interactions are blocked by an anti-SIRP α antibody (right, representative histograms).

(C) Loss of intracellular calcein red-orange in SKBR3 cells as a percentage of the control after the duration of the experiment ($n = 6$ biological replicates, 3 independent experiments).

(D and E) Kinetics of Tmab-mediated neutrophil trogocytosis quantified by flow cytometry (D) or cytotoxicity determined in parallel by 51 Cr-release (E) with either control SKBR3 cells or CD47KD SKBR3 cells. Note that the kinetics of both trogocytosis and cytotoxicity are similar and that both processes can be detected as early as 15–30 min after coincubation of effector and target cells ($n = 4$ biological replicates, 2 independent experiments). Furthermore, trogocytosis, like killing, is strictly antibody dependent, and interference with CD47-SIRP α interactions leads to enhanced trogocytosis and cytotoxicity. Statistical significance was tested with multiple t test; * $p \leq 0.05$.

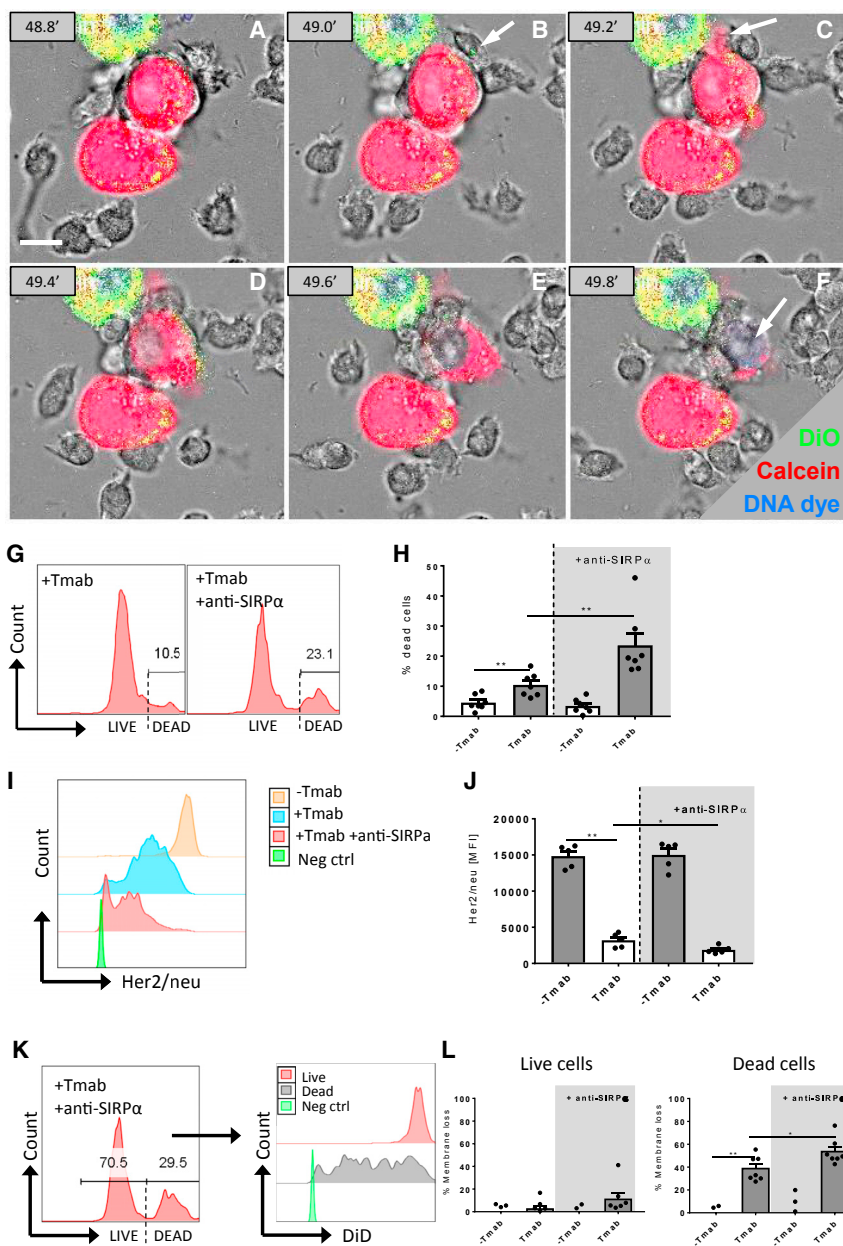


Figure 4. Trogocytosis of Tumor Cells Caused by Trogocytosis of Neutrophils during ADCC

(A–F) (A) Still images of confocal live cell imaging (taken from [Video S4](#) at the indicated times [min] after recording, which was started ~5 min after initiation of the experiment) of human neutrophils incubated with both DiO-labeled (green fluorescence) and calcein-AM-labeled (red fluorescence) SKBR3 CD47KD cells opsonized with trastuzumab (E:T ratio = 5:1). The experiment was performed in medium containing the DNA-binding dye TO-PRO3 (blue fluorescence). Scale bar represents 10 μm . Note a neutrophil (B) trogocytosing a fragment of tumor cell plasma membrane (arrow), directly followed (C, D, and E) by trogocytotic lysis (arrow), leading to permeabilization and TO-PRO3 staining of nuclear DNA (arrow) and further cytoplasmic dismantling of the cancer cell (F). Also note the yellow fluorescent dead cancer cell.

(G) Representative FACS histograms of LIVE/DEAD-violet staining of SKBR3 cells, as gated for as described in [Figure 3B](#). Gates show the percentage of SKBR3 cells that became positive for the LIVE/DEAD staining after incubation with neutrophils and the indicated conditions for 4 hr. Note that opsonizing SKBR3 cells with Tmab leads to an increase in the amount of dead SKBR3 cells and that this can be further enhanced after CD47-SIRP α checkpoint inhibition.

(H) Percentage of dead SKBR3 cells after 4-hr incubation with neutrophils, as determined by FACS in combination with LIVE/DEAD-violet staining. Results shown are averages \pm SEM from 4 independent experiments with neutrophils from 7 individual donors. Statistical significance was tested with ANOVA; ** $p \leq 0.01$.

(I) Representative histograms of Her2/neu staining on SKBR3 cells after 4-hr incubation with neutrophils.

(J) MFI values of membrane Her2/neu staining of SKBR3 cells after 4-hr incubation with neutrophils and the indicated conditions. Note the significant loss of Her2/neu staining after SKBR3 cells are opsonized with trastuzumab and incubated with neutrophils and the even greater loss of Her2/neu on trastuzumab-opsonized SKBR3 cells after incubation of the neutrophils with an anti-SIRP α antibody. Results shown are averages from 2 independent experiments with neutrophils from 5 individual donors. Statistical significance was tested with ANOVA; ** $p \leq 0.01$, * $p \leq 0.05$.

(K) Representative histogram of LIVE/DEAD-violet staining of SKBR3 cells, after opsonization with trastuzumab and 4-hr incubation with neutrophils and CD47-SIRP α block by anti-SIRP α antibody. The gating strategy for living (LIVE/DEAD-violet⁻) and dead (LIVE/DEAD-violet⁺) cells (left) is shown. Histograms for DiD staining as a representation of the amount of membrane for the gated live and dead SKBR3 cells (right).

(L) Quantification of the percentage of membrane loss in living and dead SKBR3 cells after incubation with neutrophils for 4 hr, using the gating strategy as explained in [Figures 3B](#) and [4K](#). Note that SKBR3 cells identified as dead by LIVE/DEAD staining lost the greatest amount of membrane compared to living SKBR3 cells. The percentage of membrane loss was calculated as compared to control SKBR3 cells alone. The results shown are averages \pm SEM of 3 independent experiments with neutrophils from 7 individual donors. Statistical significance was tested with ANOVA; ** $p \leq 0.01$, * $p \leq 0.05$.

with piceatannol, another inhibitor of Syk, thereby validating our screen. Further validation of a number of drugs against targets that had been implicated in neutrophil Fc γ receptor signaling ([Hawkins et al., 2010](#); [Mócsai et al., 2010](#)) revealed the involvement of intracellular Ca²⁺, phosphoinositol-3 kinase (PI3K), and the myosin light-chain kinase (MLCK) ([Figures 7D–7L](#)). This anal-

ysis demonstrated that any inhibitor of antibody-induced trogocytosis also suppressed neutrophil ADCC. In fact, until now, we had not observed any condition that prevented neutrophil trogocytosis that did not severely compromise killing. Clearly, these findings support the idea that a trogocytic process is at the base of neutrophil cytotoxicity toward cancer cells. The

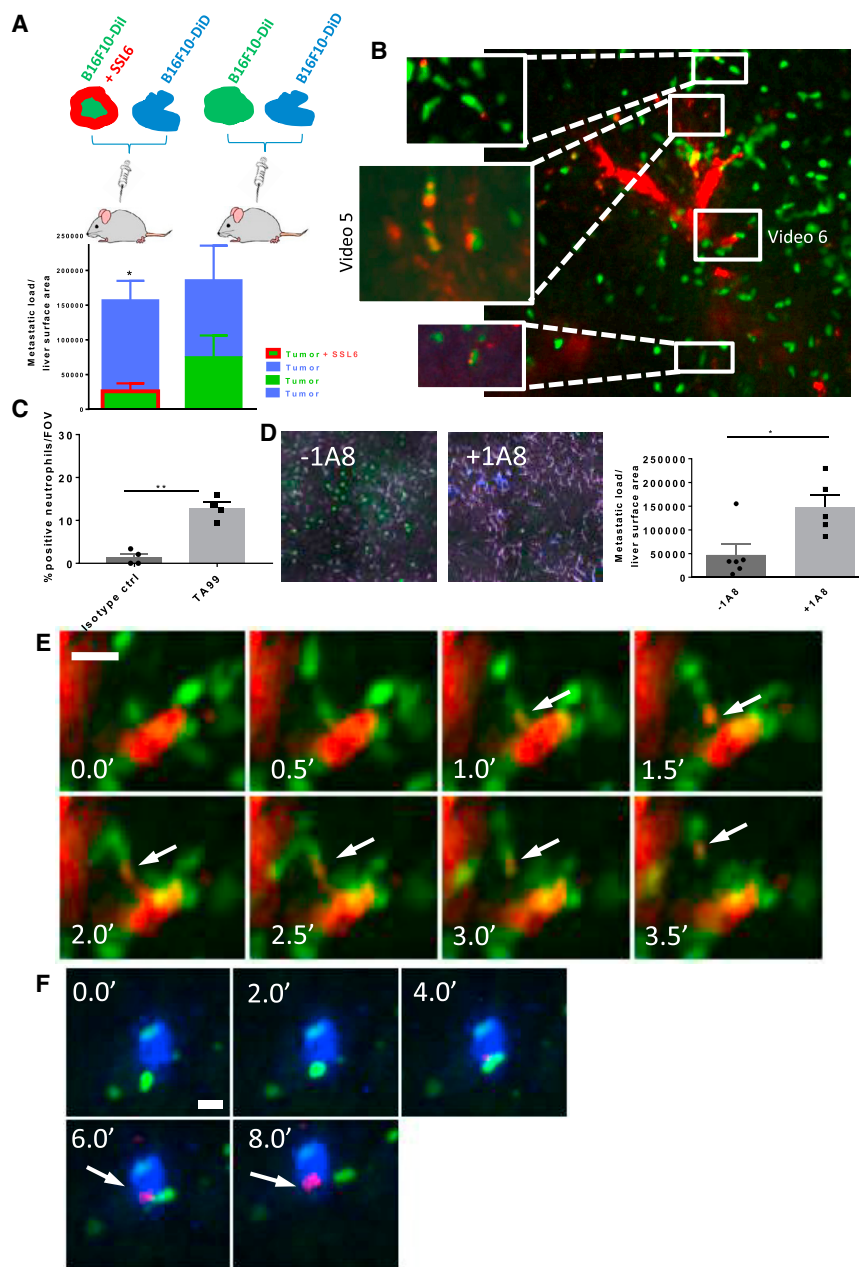


Figure 5. Neutrophil Trogoptosis Occurs In Vivo

(A) Clearance of TA99-opsized B16F10 melanoma cells *in vivo* after blocking CD47-SIRP α interactions by SSL6. Mice were injected with B16F10 melanoma cells treated or not treated with SSL6 and labeled with Dil or DiD in a 1:1 ratio, and metastatic tumor load in the liver was quantified 3 days after injection of the melanoma cells. Blocking of CD47-SIRP α interactions strongly inhibited the metastatic load of the tumor cells in the liver.

(B) Representative overview of imaging field of view in the mouse liver, showing TA99-opsized B16F10 melanoma cells (red) and neutrophils (green). As shown in the insets, numerous neutrophils can be found carrying pieces of tumor cell membrane inside (6 hr after the onset of the experiment, 10 \times objective). See also Video S5.

(C) Quantification of the amount of neutrophils positive for tumor cell membrane material (6 hr after the onset of the experiment; results shown are averages of 4 mice per group).

(D) Visual representation as measured by confocal imaging in the mouse liver of the effect of *in vivo* depletion of neutrophils by anti-Ly6G antibody. B16F10 cells (blue); neutrophils (left, green). Effect of *in vivo* depletion of neutrophils by injection of anti-Ly6G antibody 72 hr before and at the time of the start of the experiment. At that time, mice were injected with B16F10 melanoma cells, and metastatic tumor load in the liver was quantified 3 days after injection of the melanoma cells (right). Results shown are averages of 5–6 mice per group.

(E) Still images of intravital imaging in the liver of a *Lysm-egfp/Sirp α ^{d^{cyt}}* mouse, taken from Video S6 6 hr after the onset of the experiment. TA99-opsized B16F10 melanoma cells were labeled with Dil (red); neutrophils (green). As indicated by the arrows, a neutrophil can be seen actively trogocytosing a piece of membrane from the antibody-opsized tumor cell. Depletion of resident Kupffer cells using clodronate liposomes to reduce phagocytosis of tumor cells by these local macrophages permitted better visualization of neutrophil trogocytosis. Scale bar represents 25 μ m.

(F) Still images of intravital imaging in the liver of a *Lysm-egfp/Sirp α ^{d^{cyt}}* mouse, taken from Video S7 6 hr after the onset of the experiment. Neutrophils

(green); TA99-opsized B16F10 melanoma cells were labeled with DiD (blue). During the experiment, propidium iodide (PI, red) was present to detect necrotic cells. As indicated by the arrow in the still images, neutrophil-associated trogoptotic cell death is seen as shown by PI staining of nuclear DNA. Scale bar represents 25 μ m.

contribution of the different signaling components appeared roughly similar, irrespective of the presence or absence of CD47-SIRP α interactions.

DISCUSSION

Here, we describe a cellular effector mechanism by which neutrophils destroy antibody-opsized cancer cells. It is interesting

and perhaps also surprising to note that this cytotoxic mechanism, which we have termed trogoptosis (for reasons further outlined below), is essentially mechanical in nature because it causes disruption of the target cell plasma membrane, leading to a necrotic (i.e., lytic) type of cancer cell destruction. Clearly, this method of killing is different from other known mechanisms of immune cell-mediated cytotoxicity, including the apoptotic cell death that is induced by NK cells and CTLs and the

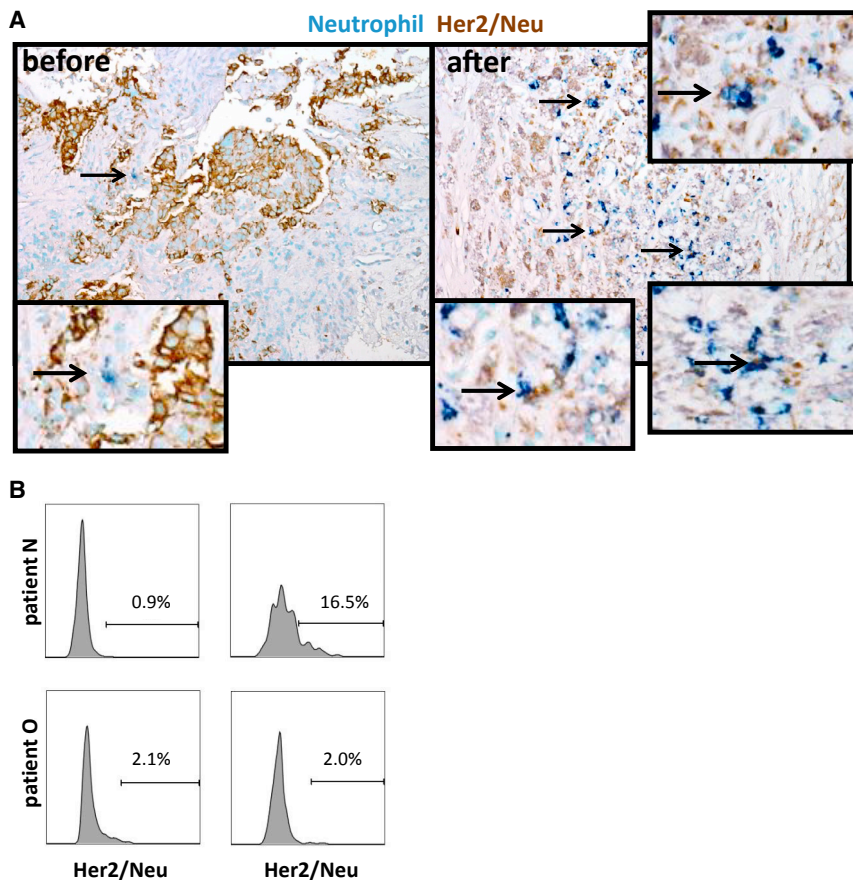


Figure 6. Tumor-Infiltrated Neutrophils of Patients with Breast Cancer Are Positive for Her2/neu, and Evaluation of Biopsies from Patients with Cancer Treated with Therapeutic Antibodies Revealed Cancer Membrane in Neutrophils

(A) Immunohistochemical analysis of biopsies of patients with breast cancer stained for MPO to detect neutrophils (blue) and Her2/neu (brown) of a patient (patient M, see table in Figure S5C) with Her2/neu⁺ breast cancer before and after neoadjuvant trastuzumab therapy.

(B) FACS analysis of breast cancer biopsies from a patient with a Her2/neu⁺ tumor (patient N, see table in Figure S5C) and from a patient with a Her2/neu⁻ tumor (patient O, see table in Figure S5C). Samples were enzymatically degraded, fixed, and permeabilized; stained for CD14 and CD33 to identify neutrophils; and stained for the presence of Her2/neu.

tent with the apparent mechanical nature of the process, which we anticipate requires pulling forces of a certain magnitude to be exerted by the neutrophil upon the target cell plasma membrane.

Our findings with human neutrophils, which also are supported by our *in vivo* intravital microscopy studies in mice, clearly fuel the idea that trogoptosis has an intimate causal relation to the well-established phenomenon of trogocytosis. That there is at least a common cause

phagocytic cell death mediated by macrophages. In particular, killing triggered by NK cells and CTLs, whether independent or dependent of antibodies and Fc γ receptor triggering, is well known to depend on granule exocytosis-dependent mechanisms (Bryceson and Long, 2008). By using cells from patients with FHL-5 lacking the munc18-2/STXBP2 protein that is known to form an absolute requirement for granule exocytosis in all leukocytes, including NK cells and neutrophils (Zhao et al., 2013), we were able to demonstrate that neutrophil ADCC is independent of granule release. Similarly, the neutrophil NADPH oxidase appeared dispensable for neutrophil ADCC, thereby showing that neutrophil ADCC toward tumor cells does not depend on the classic antimicrobial mechanisms. Furthermore, macrophages appear to use phagocytosis primarily for eliminating antibody-opsonized cancer cells (Chao et al., 2010a; Gül et al., 2014). It thus appears that trogoptosis is a mechanism of cancer cell destruction that is restricted primarily to neutrophils.

It also is clear from our current findings, which are supported by previous studies (van Spriël et al., 2001, 2003), that direct effector-target cell interactions mediated by the CD11b/CD18 integrin play a pivotal role in neutrophil cytotoxicity. In particular, CD11b/CD18 appears important for conjugate formation that in turn was shown to form a prerequisite for trogocytosis and killing. The fact that integrins, including the CD11b/CD18 integrin, mediate high-affinity interactions with their ligands is consis-

for the two phenomena is not only supported by the observations that they coincide in a spatio-temporal fashion (Figures 3 and 4; Video S4) but also because of the identical underlying mechanistic requirements, such as the integrin dependence and the various intracellular signaling events downstream of the neutrophil Fc receptor required (e.g., Figure 7). Trogocytosis has been described in the context of, for example, antigen presentation, in which T lymphocytes acquire fragments of the antigen-presenting cell plasma membrane (Joly and Hudrisier, 2003; Martínez-Martín et al., 2011; Ralston et al., 2014), but it was originally described by Tabiasco et al. (2002) to occur during NK cell cytotoxicity. However, in NK cells, trogocytosis can clearly be dissociated from the cytotoxic mechanism, which is rather granule mediated (Figure S2C; Bryceson and Long, 2008), whereas NK cell trogocytosis is not (Figure S3D). In fact, until now, trogocytosis has been essentially a phenomenon without a direct purpose in immune cell function. Notably, a study by Ralston et al. (2014) provided convincing evidence that a trogocytic mechanism exerted by the evolutionary distant parasite *E. histolytica* was causally linked to the lytic tissue damage that occurs during infection with the parasite. A more recent study provided evidence that trogocytosis is mechanistically distinct from the process of phagocytosis in the same organism (Somlata et al., 2017). Of interest, another study also demonstrated trogocytosis of antibody-opsonized cancer cells, and although this was linked to

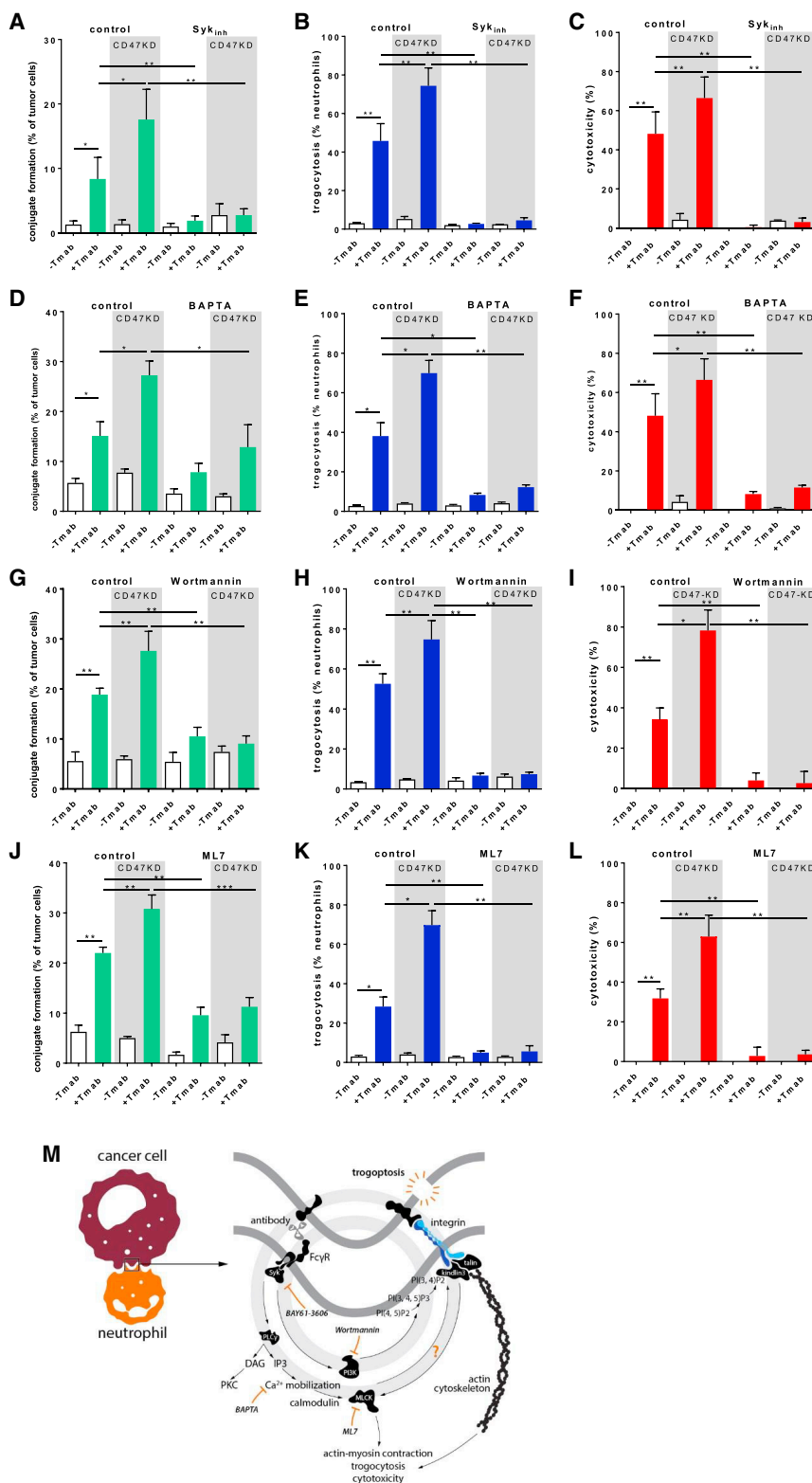


Figure 7. Signaling Downstream of Fc γ receptor Is Required for Neutrophil Trogocytosis of Antibody-Opsonized Tumor Cells.

Neutrophil conjugate formation, trogocytosis, and killing of cancer cells by trogocytosis requires signaling downstream of Fc γ receptor via the tyrosine kinase Syk (A–C), intracellular Ca²⁺ (D–F), phosphoinositide-3-kinase (PI3K) (G–I), and myosin light chain kinase (MLCK) (J–L).

(A–C) First, the role of signaling downstream of neutrophil Fc γ receptor was revealed by the use of an inhibitor of Syk (BAY61-3606; 10 μ M) on conjugate formation (A), trogocytosis (B), and cytotoxicity (C). The other indicated target signaling molecules were initially identified by screening the LOPAC library of 1,260 pharmacologically active compounds for inhibition of trogocytosis as measured by flow cytometry (also see Table S1). (D–L) Relevant targets were validated for their effects of conjugate formation (D, G, and J), trogocytosis (E, H, and K) and cytotoxicity (F, I, and L) with the indicated inhibitors (at concentrations of 10 μ M 1,2-bis[2-aminophenoxy]ethane-*N,N,N',N'*-tetraacetic acid tetrakis[acetoxymethyl ester] [BAPTA-AM]; 100 nM [Wortmannin]; 50 μ M [ML7]).

(M) Schematic representation of the Fc γ receptor signaling pathway with the signaling components involved in trogocytosis and the respective inhibitors to show their involvement (gray). The schematic representation shows a working model for the way in which Fc γ receptor signaling leads to conjugate formation, neutrophil trogocytosis, and, ultimately, to cancer cell death.

Data are averages \pm SEMs from 3–6 independent experiments that included 3–6 individual donors; statistical significance was tested with ANOVA followed by Sidak posthoc test; * $p \leq 0.05$, ** $p \leq 0.01$.

cancer cell death in the long run (during a 48-hr period), no evidence for a subsequent causally associated lytic mechanism of killing was provided (Velmurugan et al., 2016). It is worth emphasizing that, as opposed to the examples mentioned involving T cells, NK cells, and parasites, neutrophil trogocytosis is strictly dependent on the presence of antibodies directed against the tumor cells. Thus, depending on the exact conditions, trogoptosis appears to be a generic mechanism by which neutrophils destroy antibody-opsonized cancer cells, which includes both solid cancer cells, as shown herein, and hematologic cancer cells, although the exact requirements for the latter appear somewhat distinct (D.J.v.R. et al., unpublished data). Moreover, our results indicate that the trogocytosis process involves typical and well-defined signaling events downstream of Fc γ receptor in neutrophils, which include activities of the tyrosine kinase Syk, PI3K, and MLCK, as well as a role for intracellular Ca²⁺. These events are anticipated to coordinate the cytoskeletal rearrangements and the actin-myosin contraction that underlie neutrophil trogocytosis and trogoptotic cancer cell death (Figure 7M). Finally, although we believe that both phenomena (i.e., trogocytosis and trogoptosis) are essentially part of the same coordinated mechanical process that is triggered in neutrophils downstream of their Fc receptors during ADCC toward cancer cells, it does not necessarily mean that the two processes are synonymous in the sense that every single “bite” of the neutrophil directly causes lethal membrane disruption in the target cell. Our preliminary observations (H.L.M. et al., unpublished data) indicate the following: (1) it may be a proportion of the trogocytic events that leads to definitive target cell lysis, and (2) there clearly appears to be an effect of accumulation of the trogocytosis-related membrane damage to target cell death (Figures 4K and 4L), and we are investigating this relation more carefully.

One intriguing aspect of the cell death triggered by trogoptosis that we describe here is that it is essentially a lytic (i.e., necrotic) process. This means that it may not only be important for the direct destruction of antibody-opsonized cancer cells but also it may cause the release of danger-associated molecular patterns (DAMPs) and tumor (neo)antigens from the killed cancer cells. This may be instrumental in the establishment of a sterile inflammatory environment and the initiation of durable cytotoxic T cell responses, which may be important for the generation of an effective antitumor immune response (Ahrens et al., 2012; Chen and Nuñez, 2010; Matzinger, 2002; Sancho et al., 2008). What is interesting is that all of these processes may be supported positively by the targeting of CD47-SIRP α interactions, including the following: (1) as we show here, the potentiation of neutrophil trogoptosis, causing both direct killing and the release of DAMPs; (2) the enhanced removal of tumor cells by macrophages (Chao et al., 2010b); and (3) by causing an enhanced clearance and uptake of tumor material by antigen-presenting cells, which leads to improved and more effective cytotoxic T cell responses against tumors (DiLillo and Ravetch, 2015; Liu et al., 2015; Soto-Pantoja et al., 2014; Tseng et al., 2013). In line with this, it has been demonstrated that disruption of CD47-SIRP α interactions between red cells and CD4⁺ dendritic cells, respectively, also may contribute to the activation of the dendritic cells, and this may further help to generate effective

antitumor T cell immunity (van den Berg and van Bruggen, 2015; Yi et al., 2015).

One remaining question is whether neutrophil-mediated trogoptosis is relevant during other conditions (e.g., during viral infection), and this may shed light on the physiological function of neutrophil-induced trogoptosis. It is known that during infection with HIV or influenza virus, antibodies are generated that can opsonize and eliminate virus-infected cells by ADCC (Nimmerjahn et al., 2015). Neutrophils also can exert ADCC toward those cells, and it is conceivable that neutrophils also do this by trogoptosis. Finally, it is feasible that neutrophil trogoptosis plays a role in the damage to host cells during various conditions of antibody-mediated autoimmunity.

Collectively, the knowledge acquired here relating to the mechanism of neutrophil-mediated antibody-dependent destruction of cancer cells and its modulation by the CD47-SIRP α axis is likely to create additional opportunities for optimizing the clinical efficacy of antibody therapy in cancer.

STAR★METHODS

Detailed methods are provided in the online version of this paper and include the following:

- KEY RESOURCES TABLE
- CONTACT FOR REAGENT AND RESOURCE SHARING
- EXPERIMENTAL MODEL AND SUBJECT DETAILS
 - Cell Lines and Primary Cells
 - *In Vivo* Mouse Studies
- METHOD DETAILS
 - Generation of Genetically Modified Cells
 - Isolation of Effector Cells
 - Flow Cytometry experiments
 - Respiratory burst and myeloperoxidase (MPO) production during ADCC
 - Immuno electron microscopy
 - Scanning electron microscopy
 - Conjugate formation assay
 - Trogocytosis FACS assay
 - Antibody-dependent cellular cytotoxicity (ADCC)
 - Live cell imaging
 - Intravital microscopy of the liver
 - Staining of tumor samples from breast cancer patients
- QUANTIFICATION AND STATISTICAL ANALYSIS
 - Data analysis and statistics
- DATA AND SOFTWARE AVAILABILITY

SUPPLEMENTAL INFORMATION

Supplemental Information includes five figures, seven videos, and one table and can be found with this article online at <https://doi.org/10.1016/j.celrep.2018.05.082>.

ACKNOWLEDGMENTS

We are grateful to Dr. Özden Sanal (Hacettepe University, Ankara, Turkey) for providing patient material; to Ben Morris, Erik Mul, Anton Tool, and Edith van de Vijver for their help with the experiments and/or their analysis; and to Georg Kraal, Søren Moestrup, Sjaak Neefjes, and Arnoud Sonnenberg for useful discussions and for critically reading the manuscript. We also gratefully

acknowledge the contribution of Joost Bakker from SciComVisuals for graphics, including the Graphical Abstract. This research was funded in part by the Dutch Cancer Society (grant no. 10300) and the Landsteiner Research Foundation (grant no. 1223).

AUTHOR CONTRIBUTIONS

H.L.M., L.B., X.W.Z., M.v.H., D.J.v.R., L.W.T., K. Schornagel, P.V., K.F., H.J., P.H., C.L., R.L.B., and J.H.W.L. contributed to the design, execution, and evaluation of the data. J.J.B., I.K., J.v.d.W.T.B., K. Seeger, S.R., D.P., E.S., and C.W.M.-v.d.H.v.O. provided the patient material. T.M. provided the *Sirp* α^{doyt} mice. R.v.B., D.R., R.A.W.v.L., T.W.K., P.K., and T.K.v.d.B. designed the experiments and supervised the research. T.K.v.d.B. and H.L.M. wrote the manuscript.

DECLARATION OF INTERESTS

T.K.v.d.B. is the inventor of patent EP2282772 entitled “Compositions and Methods to Enhance the Immune System, which is owned by Stichting Sanquin Bloed Voorziening, relating to the targeting of CD47-SIRP α interactions in the context of antibody therapy in cancer.

Received: November 17, 2017

Revised: March 30, 2018

Accepted: May 23, 2018

Published: June 26, 2018

SUPPORTING CITATIONS

The following references appear in the Supplemental Information: Tintinger et al. (2005).

REFERENCES

- Ahrens, S., Zelenay, S., Sancho, D., Hanč, P., Kjær, S., Feest, C., Fletcher, G., Durkin, C., Postigo, A., Skehel, M., et al. (2012). F-actin is an evolutionarily conserved damage-associated molecular pattern recognized by DNGR-1, a receptor for dead cells. *Immunity* **36**, 635–645.
- Albanesi, M., Mancardi, D.A., Jönsson, F., Iannascoli, B., Fiette, L., Di Santo, J.P., Lowell, C.A., and Bruhns, P. (2013). Neutrophils mediate antibody-induced antitumor effects in mice. *Blood* **122**, 3160–3164.
- Barclay, A.N., and van den Berg, T.K. (2014). The Interaction Between Signal Regulatory Protein Alpha (SIRPalpha) and CD47: Structure, Function, and Therapeutic Target. *Annu. Rev. Immunol.* **32**, 25–50.
- Borregaard, N., Sørensen, O.E., and Theilgaard-Mönch, K. (2007). Neutrophil granules: a library of innate immunity proteins. *Trends Immunol.* **28**, 340–345.
- Bryceson, Y.T., and Long, E.O. (2008). Line of attack: NK cell specificity and integration of signals. *Curr. Opin. Immunol.* **20**, 344–352.
- Calafat, J., Janssen, H., Ståhle-Bäckdahl, M., Zuurbier, A.E., Knol, E.F., and Egesten, A. (1997). Human monocytes and neutrophils store transforming growth factor-alpha in a subpopulation of cytoplasmic granules. *Blood* **90**, 1255–1266.
- Chao, M.P., Alizadeh, A.A., Tang, C., Myklebust, J.H., Varghese, B., Gill, S., Jan, M., Cha, A.C., Chan, C.K., Tan, B.T., et al. (2010a). Anti-CD47 antibody synergizes with rituximab to promote phagocytosis and eradicate non-Hodgkin lymphoma. *Cell* **142**, 699–713.
- Chao, M.P., Jaiswal, S., Weissman-Tsakamoto, R., Alizadeh, A.A., Gentles, A.J., Volkmer, J., Weiskopf, K., Willingham, S.B., Raveh, T., Park, C.Y., et al. (2010b). Calreticulin is the dominant pro-phagocytic signal on multiple human cancers and is counterbalanced by CD47. *Sci. Transl. Med.* **2**, 63ra94.
- Chen, G.Y., and Nuñez, G. (2010). Sterile inflammation: sensing and reacting to damage. *Nat. Rev. Immunol.* **10**, 826–837.
- de Saint Basile, G., Ménasché, G., and Fischer, A. (2010). Molecular mechanisms of biogenesis and exocytosis of cytotoxic granules. *Nat. Rev. Immunol.* **10**, 568–579.
- DiLillo, D.J., and Ravetch, J.V. (2015). Differential Fc-Receptor Engagement Drives an Anti-tumor Vaccinal Effect. *Cell* **161**, 1035–1045.
- Dustin, M.L., and Long, E.O. (2010). Cytotoxic immunological synapses. *Immunol. Rev.* **235**, 24–34.
- Eruslanov, E.B., Bhojnagarwala, P.S., Quatromoni, J.G., Stephen, T.L., Ranganathan, A., Deshpande, C., Akimova, T., Vachani, A., Litzky, L., Hancock, W.W., et al. (2014). Tumor-associated neutrophils stimulate T cell responses in early-stage human lung cancer. *J. Clin. Invest.* **124**, 5466–5480.
- Fevre, C., Bestebroer, J., Mebius, M.M., de Haas, C.J., van Strijp, J.A., Fitzgerald, J.R., and Haas, P.J. (2014). Staphylococcus aureus proteins SSL6 and SEIX interact with neutrophil receptors as identified using secretome phage display. *Cell. Microbiol.* **16**, 1646–1665.
- Glennie, M.J., and van de Winkel, J.G. (2003). Renaissance of cancer therapeutic antibodies. *Drug Discov. Today* **8**, 503–510.
- Gül, N., Babes, L., Siegmund, K., Korthouwer, R., Bögels, M., Braster, R., Vi-darsson, G., ten Hagen, T.L., Kubes, P., and van Egmond, M. (2014). Macrophages eliminate circulating tumor cells after monoclonal antibody therapy. *J. Clin. Invest.* **124**, 812–823.
- Hawkins, P.T., Stephens, L.R., Suire, S., and Wilson, M. (2010). PI3K signaling in neutrophils. *Curr. Top. Microbiol. Immunol.* **346**, 183–202.
- Hernandez-Ilizaliturri, F.J., Jupudy, V., Ostberg, J., Ofazoglu, E., Huberman, A., Repasky, E., and Czuczman, M.S. (2003). Neutrophils contribute to the biological antitumor activity of rituximab in a non-Hodgkin's lymphoma severe combined immunodeficiency mouse model. *Clin. Cancer Res.* **9**, 5866–5873.
- Herrero-Turrión, M.J., Calafat, J., Janssen, H., Fukuda, M., and Mollinedo, F. (2008). Rab27a regulates exocytosis of tertiary and specific granules in human neutrophils. *J. Immunol.* **181**, 3793–3803.
- Inagaki, K., Yamao, T., Noguchi, T., Matozaki, T., Fukunaga, K., Takada, T., Hosooka, T., Akira, S., and Kasuga, M. (2000). SHPS-1 regulates integrin-mediated cytoskeletal reorganization and cell motility. *EMBO J.* **19**, 6721–6731.
- Jaiswal, S., Jamieson, C.H., Pang, W.W., Park, C.Y., Chao, M.P., Majeti, R., Traver, D., van Rooijen, N., and Weissman, I.L. (2009). CD47 is upregulated on circulating hematopoietic stem cells and leukemia cells to avoid phagocytosis. *Cell* **138**, 271–285.
- Joly, E., and Hudrisier, D. (2003). What is trogocytosis and what is its purpose? *Nat. Immunol.* **4**, 815.
- Kuijpers, K.C., Kuijpers, T.W., Zeijlemaker, W.P., Lucas, C.J., van Lier, R.A., and Miedema, F. (1990). Analysis of the role of leukocyte function-associated antigen-1 in activation of human influenza virus-specific T cell clones. *J. Immunol.* **144**, 3281–3287.
- Kuijpers, T.W., Tool, A.T., van der Schoot, C.E., Ginsel, L.A., Onderwater, J.J., Roos, D., and Verhoeven, A.J. (1991). Membrane surface antigen expression on neutrophils: a reappraisal of the use of surface markers for neutrophil activation. *Blood* **78**, 1105–1111.
- Liu, X., Pu, Y., Cron, K., Deng, L., Kline, J., Frazier, W.A., Xu, H., Peng, H., Fu, Y.X., and Xu, M.M. (2015). CD47 blockade triggers T cell-mediated destruction of immunogenic tumors. *Nat. Med.* **21**, 1209–1215.
- Majeti, R., Chao, M.P., Alizadeh, A.A., Pang, W.W., Jaiswal, S., Gibbs, K.D., Jr., van Rooijen, N., and Weissman, I.L. (2009). CD47 is an adverse prognostic factor and therapeutic antibody target on human acute myeloid leukemia stem cells. *Cell* **138**, 286–299.
- Martinez-Martin, N., Fernández-Arenas, E., Cemerski, S., Delgado, P., Turner, M., Heuser, J., Irvine, D.J., Huang, B., Bustelo, X.R., Shaw, A., and Alarcón, B. (2011). T cell receptor internalization from the immunological synapse is mediated by TC21 and RhoG GTPase-dependent phagocytosis. *Immunity* **35**, 208–222.
- Matzinger, P. (2002). The danger model: a renewed sense of self. *Science* **296**, 301–305.
- Meeths, M., Entesarian, M., Al-Herz, W., Chiang, S.C., Wood, S.M., Al-Ateeqi, W., Almazan, F., Boelens, J.J., Hasle, H., Iversen, M., et al. (2010). Spectrum of clinical presentations in familial hemophagocytic lymphohistiocytosis type 5 patients with mutations in STXBP2. *Blood* **116**, 2635–2643.

- Mócsai, A., Ruland, J., and Tybulewicz, V.L. (2010). The SYK tyrosine kinase: a crucial player in diverse biological functions. *Nat. Rev. Immunol.* *10*, 387–402.
- Montalvo, F., Garcia, Z., Celli, S., Breart, B., Deguine, J., Van Rooijen, N., and Bousso, P. (2013). The mechanism of anti-CD20-mediated B cell depletion revealed by intravital imaging. *J. Clin. Invest.* *123*, 5098–5103.
- Musolino, A., Naldi, N., Bortesi, B., Pezzuolo, D., Capelletti, M., Missale, G., Laccabue, D., Zerbini, A., Camisa, R., Bisagni, G., et al. (2008). Immunoglobulin G fragment C receptor polymorphisms and clinical efficacy of trastuzumab-based therapy in patients with HER-2/neu-positive metastatic breast cancer. *J. Clin. Oncol.* *26*, 1789–1796.
- Nimmerjahn, F., and Ravetch, J.V. (2008). Fcγ receptors as regulators of immune responses. *Nat. Rev. Immunol.* *8*, 34–47.
- Nimmerjahn, F., Gordan, S., and Lux, A. (2015). FcγR dependent mechanisms of cytotoxic, agonistic, and neutralizing antibody activities. *Trends Immunol.* *36*, 325–336.
- Oldham, R.K., and Dillman, R.O. (2008). Monoclonal antibodies in cancer therapy: 25 years of progress. *J. Clin. Oncol.* *26*, 1774–1777.
- Ralston, K.S., Solga, M.D., Mackey-Lawrence, N.M., Somlata, Bhattacharya, A., and Petri, W.A., Jr. (2014). Trophocytosis by *Entamoeba histolytica* contributes to cell killing and tissue invasion. *Nature* *508*, 526–530.
- Reeves, E.P., Lu, H., Jacobs, H.L., Messina, C.G., Bolsover, S., Gabella, G., Potma, E.O., Warley, A., Roes, J., and Segal, A.W. (2002). Killing activity of neutrophils is mediated through activation of proteases by K⁺ flux. *Nature* *416*, 291–297.
- Ring, N.G., Herndler-Brandstetter, D., Weiskopf, K., Shan, L., Volkmer, J.P., George, B.M., Lietzenmayer, M., McKenna, K.M., Naik, T.J., McCarty, A., et al. (2017). Anti-SIRPα antibody immunotherapy enhances neutrophil and macrophage antitumor activity. *Proc. Natl. Acad. Sci. USA* *114*, E10578–E10585.
- Roos, D., van Bruggen, R., and Meischl, C. (2003). Oxidative killing of microbes by neutrophils. *Microbes Infect.* *5*, 1307–1315.
- Rosseau, S., Selhorst, J., Wiechmann, K., Leissner, K., Maus, U., Mayer, K., Grimminger, F., Seeger, W., and Lohmeyer, J. (2000). Monocyte migration through the alveolar epithelial barrier: adhesion molecule mechanisms and impact of chemokines. *J. Immunol.* *164*, 427–435.
- Sancho, D., Mourão-Sá, D., Joffre, O.P., Schulz, O., Rogers, N.C., Pennington, D.J., Carlyle, J.R., and Reis e Sousa, C. (2008). Tumor therapy in mice via antigen targeting to a novel, DC-restricted C-type lectin. *J. Clin. Invest.* *118*, 2098–2110.
- Segal, A.W. (2005). How neutrophils kill microbes. *Annu. Rev. Immunol.* *23*, 197–223.
- Siders, W.M., Shields, J., Garron, C., Hu, Y., Boutin, P., Shankara, S., Weber, W., Roberts, B., and Kaplan, J.M. (2010). Involvement of neutrophils and natural killer cells in the anti-tumor activity of alemtuzumab in xenograft tumor models. *Leuk. Lymphoma* *51*, 1293–1304.
- Somlata, N.-T., Nakada-Tsukui, K., and Nozaki, T. (2017). AGC family kinase 1 participates in trophocytosis but not in phagocytosis in *Entamoeba histolytica*. *Nat. Commun.* *8*, 101.
- Soto-Pantoja, D.R., Miller, T.W., Frazier, W.A., and Roberts, D.D. (2012). Inhibitory signaling through signal regulatory protein-α is not sufficient to explain the antitumor activities of CD47 antibodies. *Proc. Natl. Acad. Sci. USA* *109*, E2842–E2845, author reply E2844–E2845.
- Soto-Pantoja, D.R., Terabe, M., Ghosh, A., Ridnour, L.A., DeGraff, W.G., Wink, D.A., Berzofsky, J.A., and Roberts, D.D. (2014). CD47 in the tumor microenvironment limits cooperation between antitumor T-cell immunity and radiotherapy. *Cancer Res.* *74*, 6771–6783.
- Strome, S.E., Sausville, E.A., and Mann, D. (2007). A mechanistic perspective of monoclonal antibodies in cancer therapy beyond target-related effects. *Oncologist* *12*, 1084–1095.
- Suzuki, E., Kataoka, T.R., Hirata, M., Kawaguchi, K., Nishie, M., Haga, H., and Toi, M. (2015). Trophocytosis-mediated expression of HER2 on immune cells may be associated with a pathological complete response to trastuzumab-based primary systemic therapy in HER2-overexpressing breast cancer patients. *BMC Cancer* *15*, 39.
- Tabiasco, J., Espinosa, E., Hudrisier, D., Joly, E., Fournié, J.J., and Vercellone, A. (2002). Active trans-synaptic capture of membrane fragments by natural killer cells. *Eur. J. Immunol.* *32*, 1502–1508.
- Taylor, R.P., and Lindorfer, M.A. (2015). Fcγ-receptor-mediated trophocytosis impacts mAb-based therapies: historical precedence and recent developments. *Blood* *125*, 762–766.
- Tintinger, G., Steel, H.C., and Anderson, R. (2005). Taming the neutrophil: calcium clearance and influx mechanisms as novel targets for pharmacological control. *Clin. Exp. Immunol.* *141*, 191–200.
- Topalian, S.L., Drake, C.G., and Pardoll, D.M. (2015). Immune checkpoint blockade: a common denominator approach to cancer therapy. *Cancer Cell* *27*, 450–461.
- Treffers, L.W., Zhao, X.W., van der Heijden, J., Nagelkerke, S.Q., van Rees, D.J., Gonzalez, P., Geissler, J., Verkuijlen, P., van Houdt, M., de Boer, M., et al. (2018). Genetic variation of human neutrophil Fcγ receptors and SIRPα in antibody-dependent cellular cytotoxicity towards cancer cells. *Eur. J. Immunol.* *48*, 344–354.
- Tseng, D., Volkmer, J.P., Willingham, S.B., Contreras-Trujillo, H., Fathman, J.W., Fernhoff, N.B., Seita, J., Inlay, M.A., Weiskopf, K., Miyanishi, M., and Weissman, I.L. (2013). Anti-CD47 antibody-mediated phagocytosis of cancer by macrophages primes an effective antitumor T-cell response. *Proc. Natl. Acad. Sci. USA* *110*, 11103–11108.
- Valgardsdottir, R., Cattaneo, I., Klein, C., Introna, M., Figliuzzi, M., and Golay, J. (2017). Human neutrophils mediate trophocytosis rather than phagocytosis of CLL B cells opsonized with anti-CD20 antibodies. *Blood* *129*, 2636–2644.
- van Beek, E.M., Zarate, J.A., van Bruggen, R., Schornagel, K., Tool, A.T., Matozaki, T., Kraal, G., Roos, D., and van den Berg, T.K. (2012). SIRPα controls the activity of the phagocyte NADPH oxidase by restricting the expression of gp91(phox). *Cell Rep.* *2*, 748–755.
- van Egmond, M., and Bakema, J.E. (2013). Neutrophils as effector cells for antibody-based immunotherapy of cancer. *Semin. Cancer Biol.* *23*, 190–199.
- van de Vijver, E., Maddalena, A., Sanal, Ö., Holland, S.M., Uzel, G., Madhakar, M., de Boer, M., van Leeuwen, K., Köker, M.Y., Parvaneh, N., et al. (2012). Hematologically important mutations: leukocyte adhesion deficiency (first update). *Blood Cells Mol. Dis.* *48*, 53–61.
- van den Berg, T.K., and van Bruggen, R. (2015). Loss of CD47 makes dendritic cells see red. *Immunity* *43*, 622–624.
- van Spruiel, A.B., Leusen, J.H., van Egmond, M., Dijkman, H.B., Assmann, K.J., Mayadas, T.N., and van de Winkel, J.G. (2001). Mac-1 (CD11b/CD18) is essential for Fc receptor-mediated neutrophil cytotoxicity and immunologic synapse formation. *Blood* *97*, 2478–2486.
- van Spruiel, A.B., van Ojik, H.H., Bakker, A., Jansen, M.J., and van de Winkel, J.G. (2003). Mac-1 (CD11b/CD18) is crucial for effective Fc receptor-mediated immunity to melanoma. *Blood* *101*, 253–258.
- Velmurugan, R., Challa, D.K., Ram, S., Ober, R.J., and Ward, E.S. (2016). Macrophage-Mediated Trophocytosis Leads to Death of Antibody-Opsonized Tumor Cells. *Mol. Cancer Ther.* *15*, 1879–1889.
- Weiskopf, K., Ring, A.M., Ho, C.C., Volkmer, J.P., Levin, A.M., Volkmer, A.K., Ozkan, E., Fernhoff, N.B., van de Rijn, M., Weissman, I.L., and Garcia, K.C. (2013). Engineered SIRPα variants as immunotherapeutic adjuvants to anti-cancer antibodies. *Science* *341*, 88–91.
- Yi, T., Li, J., Chen, H., Wu, J., An, J., Xu, Y., Hu, Y., Lowell, C.A., and Cyster, J.G. (2015). Splenic Dendritic Cells Survey Red Blood Cells for Missing Self-CD47 to Trigger Adaptive Immune Responses. *Immunity* *43*, 764–775.
- Zhao, X.W., van Beek, E.M., Schornagel, K., van der Maaden, H., van Houdt, M., Otten, M.A., Finetti, P., van Egmond, M., Matozaki, T., Kraal, G., et al. (2011). CD47-signal regulatory protein-α (SIRPα) interactions form a barrier for antibody-mediated tumor cell destruction. *Proc. Natl. Acad. Sci. USA* *108*, 18342–18347.

Zhao, X.W., Kuijpers, T.W., and van den Berg, T.K. (2012a). Is targeting of CD47-SIRP α enough for treating hematopoietic malignancy? *Blood* 119, 4333–4334, author reply 4334–4335.

Zhao, X.W., Matlung, H.L., Kuijpers, T.W., and van den Berg, T.K. (2012b). On the mechanism of CD47 targeting in cancer. *Proc. Natl. Acad. Sci. USA* 109, E2843, author reply E2844–E2845.

Zhao, X.W., Gazendam, R.P., Drewniak, A., van Houdt, M., Tool, A.T., van Hamme, J.L., Kustiawan, I., Meijer, A.B., Janssen, H., Russell, D.G., et al.

(2013). Defects in neutrophil granule mobilization and bactericidal activity in familial hemophagocytic lymphohistiocytosis type 5 (FHL-5) syndrome caused by STXBP2/Munc18-2 mutations. *Blood* 122, 109–111.

Zhu, E.F., Gai, S.A., Opel, C.F., Kwan, B.H., Surana, R., Mihm, M.C., Kauke, M.J., Moynihan, K.D., Angelini, A., Williams, R.T., et al. (2015). Synergistic innate and adaptive immune response to combination immunotherapy with anti-tumor antigen antibodies and extended serum half-life IL-2. *Cancer Cell* 27, 489–501.

STAR★METHODS

KEY RESOURCES TABLE

REAGENT or RESOURCE	SOURCE	IDENTIFIER
Antibodies		
Anti-CD11b, clone 44A	ATCC	Cat# ATCC HB-249; RRID:CVCL_J601
Anti-CD18, clone IB4	ATCC	Cat# ATCC HB-10164; RRID: CVCL_0339
CLB-LFA1/2	Sanquin	Cat# M1385 P35
Anti-CD11c	Rosseau et al., 2000	N/A
Monovalent human Fc fragments	Bethyl	Cat# A80-104AP; RRID: AB_67062
Anti-CD32 F(ab') ₂ , clone 7.3	Ancell	Cat# 181-520
Anti-CD16 F(ab') ₂ , clone 3G8	Ancell	Cat# 165-520
Anti-CD47 F(ab') ₂ , clone B6H12	Zhao et al., 2011	N/A
Anti-SIRP α , clone 12C4	Zhao et al., 2011	N/A
Anti-MPO	Herrero-Turrión et al., 2008	N/A
Anti-Lactoferrin	Herrero-Turrión et al., 2008	N/A
Anti-CD33-PE, clone WM53	BD Biosciences	Cat# 555450; RRID: AB_395843
Anti-CD14-PE-Cy7, clone M5E2	Biolegend	Cat# 301813; RRID: AB_389352
Anti-CD340-APC, clone 24D2	Biolegend	Cat# 324407; RRID: AB_756123
Anti-HER2, clone 4B5	Roche	Cat# 790-2991; RRID: AB_2335975
Anti-GR1, clone 1A8	BioXcell	Cat# BE0075-1; RRID: AB_1107721
Trastuzumab	Roche	N/A
Cetuximab	Merck KGaA	N/A
TA99	BioXcell	Cat# BE0151; RRID: AB_10949462
Chemicals, Peptides, and Recombinant Proteins		
Anti-APC MACS beads	Miltenyi	Cat# 130-090-855; RRID: AB_244367
Anti-CD56 MACS beads	Miltenyi	Cat# 130-050-401
Liberase TM	Roche	Cat# 00000005401119001
Intraprep kit	Beckman Coulter	Cat# A07803
G-CSF	Neupogen	N/A
IFN γ	PEPROTECH	Cat# 300-02
LIVE/DEAD viability kit	ThermoFisher	Cat# L34955
Lipophilic membrane dyes (DiO, DiD)	Invitrogen	Cat# V22886, V22887
Library of Pharmacologically Active Compounds (LOPAC)	Sigma-Aldrich	Cat# LO4100
TO-PRO-3 iodide	Invitrogen	Cat# T3605
Calcein-AM green / red-orange	Invitrogen	Cat# C34852, C34851
Syk inhibitor: BAY 61-3606	Sigma	Cat# B9685-5MG
PI3K inhibitor: Wortmannin	Sigma	Cat# 12-338
MLCK inhibitor: ML7	Sigma	Cat# I2764-5MG
Critical Commercial Assays		
Amplex Red assay	Molecular Probes	Cat# A22188
MPO ELISA	Hycult	Cat# HK324-02; RRID: AB_10989641
Experimental Models: Cell Lines		
Human: SKBR3	ATCC	Cat# HTB-30; RRID:CVCL_0033
Human: A431	ATCC	Cat# CRL-1555; RRID:CVCL_0037
Mouse: B16F10	ATCC	Cat# CRL-6475; RRID:CVCL_0159
Human: HEK293T	ATCC	Cat#: ATCC CRL-3216; RRID: CVCL_0063

(Continued on next page)

Continued		
REAGENT or RESOURCE	SOURCE	IDENTIFIER
Experimental Models: Organisms/Strains		
Mice: Lysm-egfp	Dr. T. Graf	N/A
Mice: Lysm-egfp/SIRP α Δ cyt	Inagaki et al., 2000	N/A
Oligonucleotides		
shRNA targeting sequence: CD47: 5'CCGGGCACAA-TTACTTGGACTAGTTCTCGAGAAGTAGTCCAAGTAATTGTGCTTTTT-3'	Zhao et al., 2011	N/A
Software and Algorithms		
Prism 7	Graphpad	N/A
FloJo v10	Tree Star	N/A
ImageJ	NIH	N/A
Velocity	Perkin-Elmer	N/A

CONTACT FOR REAGENT AND RESOURCE SHARING

Further information and requests for resources and reagents should be directed to and will be fulfilled by the Lead Contact, Timo van den Berg (t.k.vandenberg@sanquin.nl).

EXPERIMENTAL MODEL AND SUBJECT DETAILS

Cell Lines and Primary Cells

The Her2/neu-positive human breast cancer cell line SKBR3 (source: female) was routinely cultured in IMDM medium supplemented with 20% (v/v) fetal bovine serum, 2 mM L-glutamine, 100 U/ml penicillin and 100 μ g/ml streptomycin at 37°C and 5% CO₂. The human epidermoid carcinoma cell line A431 (source: female) was routinely cultured in RPMI 1640 medium supplemented with 10% (v/v) fetal bovine serum, 2 mM L-glutamine, 100 U/ml penicillin and 100 μ g/ml streptomycin at 37°C and 5% CO₂. Primary neutrophils or NK cells, isolated from healthy donors or from Familial Hemophagocytic Lymphadenocytosis type 5 (FHL5) patients, Chronic Granulomatous Disease (CGD) patients, LAD-I patients and LAD-III patients were used (see [Figure S1E](#) for patient details). Blood was collected after informed consent and according to the Declaration of Helsinki 1964. Studies on human blood samples were approved by the Sanquin Research institutional medical ethical committee. After isolation (see [Methods](#) section below for a detailed protocol), neutrophils were cultured for either 4 hr or overnight in RPMI 1640 culture medium, supplemented with 10% (v/v) fetal bovine serum, 2 mM L-glutamine, 100 U/ml penicillin and 100 μ g/ml streptomycin, in the presence of 10 ng/ml clinical grade recombinant G-CSF and 50 ng/ml recombinant human interferon- γ at a concentration of 5x10⁶ cells/ml. The use of unstimulated neutrophils in trogocytosis and ADCC assays lead to similar results, although the overall response was in general lower (data not shown). NK cells were cultured overnight in RPMI 1640 culture medium, supplemented with 10% (v/v) FCS, 100 U/ml penicillin, 100 μ g/ml streptomycin, and 1% (v/v) L-glutamine, at a concentration of 5x10⁶ cells/ml.

Mouse neutrophils from C57BL/6J mice were isolated according to isolation protocol described below. After isolation, mouse neutrophils were cultured overnight in RPMI 1640 culture medium, supplemented with 10% (v/v) FCS, 100 U/ml penicillin, 100 μ g/ml streptomycin, and 1% (v/v) L-glutamine, in the presence of 10 ng/ml clinical grade recombinant G-CSF and 50 ng/ml recombinant murine interferon- γ at a concentration of 5x10⁶ cells/ml.

In Vivo Mouse Studies

Male and female 8-12 weeks old Lysm-egfp knockin reporter mice (Dr. T. Graf, Albert Einstein College, New York) and *Lysm-egfp/Sirp α Δ cyt* mice (Inagaki et al., 2000) were housed at 20-25°C, 50%–60% humidity with a 12/12 light/dark cycle in the Animal Health Unit at The University of Calgary (Calgary, Canada), and all procedures were approved by The University of Calgary Institutional Animal Care and Use Committee. For all *in vivo* imaging studies, after tumors were injected, mice were randomly assigned to experimental groups.

METHOD DETAILS

Generation of Genetically Modified Cells

CD47 was knocked down in SKBR3 cells with shRNA (5'CCGGGCACAA-TTACTTGGACTAGTTCTCGAGAAGTAGTCCAAGTAATTGTGCTTTTT-3'; referred to as SKBR3 CD47KD cells), resulting in 10%–15% expression of normal CD47 surface levels as

shown previously.(Zhao et al., 2011) Knock-down of CD47 was routinely verified by flow cytometry and was found to be stable over periods upto 6 months in culture (see Figure S4G). SKBR3 cells expressing empty vector shRNA were used as control. For overexpression of lamin B-GFP in SKBR3 cells, the coding sequence of full-length lamin B1 was cloned into the lentiviral vector pRRL PPT SFFV GFP prester SIN. Lentiviral particles were produced in HEK293T cells which were transient cotransfected with the lentiviral vector, pMDLgp, RSVrev and pCMV-VSVg. On day 2 and 3 after transfection, virus containing supernatant was harvested and directly added to WT SKBR3 cells after filtering through a 0,45 μ M filter. GFP-positive cells were selected by flow cytometry sorting before their use on further assays.

For overexpression of mouse CD47, the coding sequence of mouse CD47 was cloned into pENTR-d-TOPO; this construct was recombined with pLenti6.3/V5-DEST by LR Clonase II (Invitrogen) to obtain pLenti6.3-mCD47. SKBR3 CD47KD cells were lentivirally transduced with pLenti6.3-mCD47, as described for the CD47 knockdown construct(Zhao et al., 2011), followed by positive selection with blasticidin. A431 cells expressing human Her2/Neu were generated by retroviral transduction, followed by positive selection using puromycin.

Isolation of Effector Cells

Neutrophils (PMNs) were isolated as previously described.(Kuijpers et al., 1991) Briefly, granulocytes were isolated by density gradient centrifugation with isotonic Percoll and erythrocyte lysis. NK cells were isolated from the PBMC fraction of blood after Percoll fractionation by means of anti-CD56-coated MACS beads, according to procedures provided by the manufacturer. Mouse neutrophils from C57BL/6J mice were isolated with anti-GR1 antibody coupled to APC (clone 1A8, concentration 1:200) and anti-APC MACS beads, according to the procedures provided by the manufacturer.

Flow Cytometry experiments

In FACS analysis of tumor samples from breast cancer patients (see Figures S5C and S5D) neutrophils were identified by positive staining for CD33 and negative staining for CD14. In these samples, Her2/neu was stained by use of anti-CD340 antibody. Briefly, solid tumor samples were minced and enzymatically degraded into single cell suspensions by incubating at 37°C in HEPES dissociation buffer containing Liberase TM (Roche, 125 μ g/ml) for 1 hr. Single cell suspensions were washed in HEPES buffer, fixed and permeabilized using intraprep kit (Beckman Coulter) according to protocol provided by the manufacturer, and stained with the mentioned antibodies, after which the cells were measured on a LSRII flow cytometer (BD Biosciences).

Respiratory burst and myeloperoxidase (MPO) production during ADCC

NADPH oxidase activity was evaluated during ADCC by measuring extracellular hydrogen peroxide release in an Amplex Red assay (Molecular Probes) as previously described.(van Beek et al., 2012) Samples were measured in the presence of Amplex Red (0.5 μ M) and horseradish peroxidase (1 U/ml). Fluorescence was measured on a plate reader (TECAN) and maximal slope was determined over a 2-minute interval to calculate NADPH oxidase activity. MPO release from PMNs during ADCC of cancer cells was measured by ELISA (Hycult), according to protocol of the manufacturer.

Immuno electron microscopy

Conjugate formation and trogocytosis of PMNs and tumor cells were visualized by electron microscopy. Briefly, 1×10^6 /ml SKBR3 cells were labeled with biotin (concentration 0.01 mg/ml, EZ Link Sulfo NHS Biotin, ThermoFisher) by incubation in HEPES- buffer at 37°C for 30 min. Thereafter, 10×10^6 human neutrophils were coincubated with 2×10^6 target cells (E:T ratio = 5:1) in the absence or presence of 10 μ g/ml trastuzumab (Roche) for the indicated times at 37°C in a 5% CO₂ atmosphere to allow conjugate formation to occur. Cells were fixed in 2% paraformaldehyde + 0.2% glutaraldehyde in 0.1 M PHEM buffer (60 mM PIPES, 25 mM HEPES, 2 mM MgCl₂, 10 mM EGTA, pH 6.9) and then processed for ultrathin cryosectioning as previously described.(Calafat et al., 1997) Briefly, 60-nm cryosections were cut at -120°C with diamond knives in a cryoultramicrotome (Leica Aktiengesellschaft, Vienna, Austria) and transferred with a mixture of sucrose and methylcellulose onto formvarcoated copper grids. The grids were placed on 35-mm Petri dishes containing 2% (w/v) gelatine. Ultrathin frozen sections were incubated at room temperature with polyclonal antibodies either against MPO (1/14,000) or lactoferrin (1/1,200) followed by 10-nm protein A-conjugated colloidal gold (EM Lab, Utrecht University, Netherlands) as first marker. To block protein A binding sites the sections were fixed for 10 min. with 1% (w/v) glutaraldehyde, then a polyclonal antibody against biotin (1/20,000) incubation, marked by 15- nm protein A-conjugated colloidal gold (EM Lab, Utrecht University, Netherlands). After immuno labeling, the sections were embedded in a mixture of methylcellulose and uranyl acetate and examined with a Philips CM10 electron microscope (FEI company, Eindhoven, the Netherlands).

Scanning electron microscopy

SKBR3 cells were cultured on glass coverslips (13 mm). PMNs were added in E:T ratio 5:1 for 45 min in the presence of 5 μ g/ml Trastuzumab. Cells were fixed with McDowell's Trumps Fixative. Water was removed from the samples with increasing concentrations ethanol and dried in a desiccator. Samples were examined with a Phenom scanning electron microscope (FEI company, Eindhoven, the Netherlands).

Conjugate formation assay

A total of 1×10^6 G-CSF/IFN γ -primed human neutrophil effector cells labeled with CellTrace calcein violet-AM fluorescent dye (Invitrogen, Grand Island, NY, USA) were incubated with 2×10^5 SKBR3 cells stained with CMTPX/cell-tracker red fluorescent dye (Invitrogen) (E:T ratio = 5:1) in the absence or presence of 5 μ g/ml Trastuzumab for 30 min at 37°C in 5% CO $_2$. After incubation, the cells were fixed with 1.2% (w/v) paraformaldehyde in PBS. Samples were run in an ImageStreamX flow cytometer (Amnis Corporation, Seattle, WA, USA) and images were acquired for 10,000 events/sample. Cell images of double-positive events CMTPX $^+$ /Calcein $^+$ were analyzed to visualize and quantify effector-target cell conjugate formation with the Amnis' IDEAS $^{\text{®}}$ data analysis package.

Trogocytosis FACS assay

The transfer of membrane from tumor cell to neutrophil was quantified by flow cytometry. Membranes of tumor target cells were labeled with lipophilic membrane dye (DiO, 5 μ M, Invitrogen; DiI, 5 μ M, Invitrogen) for 30 min at 37°C. After washing with PBS, cells were incubated together with neutrophils in a U-bottom 96-well plate at a E:T ratio of 5:1 or in the absence or presence of 5 μ g/ml trastuzumab (Roche) or 2 μ g/ml cetuximab (Merck KGaA). Samples were fixed with stopbuffer containing 0.5% (w/v) PFA, 1% (w/v) BSA and 20mM NaF at several time points between 0 and 120 min and measured on a FACS. After gating for the neutrophil population, based on SSC and a nuclear marker (stable lamin B-GFP expression) in the target cells (see also Figure 3B), the mean fluorescent intensity (MFI) and the percentage of cells positive for DiO/DiI were evaluated. For measuring both trogocytosis and ADCC at the same time by flow cytometry, lamin-GFP expressing SKBR3 target cells were labeled with a lipophilic membrane dye (DiI), a cytoplasmic dye (calcein red-orange) and incubated with neutrophils for 4 hr in the absence or presence of 5 μ g/ml trastuzumab. After the incubation period, cells were washed and stained for dead cells by use of a LIVE/DEAD viability kit (ThermoFisher). Afterward, samples were washed and fixed with stopbuffer containing 0.5% (w/v) PFA, 1% (w/v) BSA and 20mM NaF and measured on FACS.

Controls and CD47-SIRP α interference in trogocytosis assay

Control experiments were carried out where target cells had been labeled with either biotin, or where trastuzumab itself was labeled with a fluorescent label by the use of Lightning Link Conjugation kit (Innova Biosciences) (see Figure S4H). Alternatively, the plasma membrane had been genetically labeled by transfection of the target cells with a GFP-CAAX construct, which expresses an N-terminal GFP-tagged tetra-amino acid motif (CAAX), localizing GFP to the plasma membrane. These experiments showed similar results compared to labeling the target cell with lipophilic membrane dye. In indicated experiments, CD47-SIRP α interactions were inhibited, either by use of anti-CD47 F(ab') $_2$, anti-SIRP α antibody, or by knockdown of CD47 in target cells, as stated in the legends of the Figures.

Compound Screening in Trogocytosis assay

To further evaluate the mechanistic pathway involved in trogocytosis, we made use of our FACS-based trogocytosis assay as described above, in combination with the Library of Pharmacologically Active Compounds (LOPAC, Sigma-Aldrich), consisting of 1280 compounds with described pharmacological actions, including kinase inhibitors, receptor ligands, and approved drugs. All compounds in this library were used in a concentration of 10 μ M. As controls on each 96-well plate, SKBR3 cells and SKBR3 CD47KD cells were incubated together with PMNs either in the absence or presence of trastuzumab. The normalization method used was Normalized Percent Inhibition. The LOPAC library was screened with three biological replicates and was further analyzed both by MFI and by percentage positive PMNs. Hits were defined as over 80% inhibition of membrane transfer from tumor cells to PMNs as measured by FACS.

Hits found by use of the LOPAC library were validated on conjugate formation assay, trogocytosis assay and ADCC assay, and included inhibitors of Syk kinase (BAY 61-3606), myosin light chain kinase (ML7) and PI3K (Wortmannin).

Antibody-dependent cellular cytotoxicity (ADCC)

Target cells were labeled with 100 μ Ci 51 Cr (Perkin-Elmer) for 90 min at 37°C. After 3 washes with PBS, in indicated experiments, CD47-SIRP α interactions were blocked by incubating SKBR3 cells or SKBR3 CD47KD msCD47KI cells (1×10^6) with 10 μ g of SSL6 (kind gift from J.A. van Strijp and P.J.A. Haas, Utrecht, the Netherlands) for 30 min on ice. After 2 washes with PBS, 5×10^3 cells were incubated in RPMI culture medium supplemented with 10% (v/v) FCS for 4 hr at 37°C and 5% CO $_2$ in a 96-well U-bottom plate together with PMNs in a E:T ratio of 50:1 in the presence of the appropriate antibodies. After the incubation of target cells and effector cells, supernatant was harvested and analyzed for radioactivity in a gamma counter (Wallac). The percentage of cytotoxicity was calculated as [(experimental cpm- spontaneous cpm)/ (total cpm- spontaneous cpm)] x 100%. All conditions were measured in triplicate. To visualize target cells after ADCC assay, effector cells were incubated with target cells for 4 hr at 37°C (T:E ratio 1:5 for NK cells; T:E ratio 1:50 for PMNs), after which cytopspins were made of 30,000- 60,000 total cells in a cytocentrifuge (Cytospin 4, Shandon).

For integrin blocking experiments mAbs 44A and IB4 against CD11b/CD18 were pre-incubated either separately or together with PMNs at 10 μ g/ml each for 10 min, after which the cells were used in ADCC, trogocytosis and conjugate formation experiments. Other integrins were blocked with CLB-LFA1/2 (Sanquin, the Netherlands), anti-CD11a(Kuijpers et al., 1990), CBR-p150/4G1 (AbD Serotec) and anti-CD11c(Rosseau et al., 2000), which were also used at 10 μ g/ml in a similar fashion. For blocking Fc γ receptors, a

combination of monovalent human Fc fragments to block Fc γ RI (CD64), mAb 7.3 against Fc γ RII (CD32), and mAb 3G8 against Fc γ RIII (CD16) were pre-incubated with PMNs for 20 min at a concentration of 10 μ g/ml, after which cells were used in conjugate formation and ADCC experiments. An appropriate isotype control (Ancell) was used as control condition.

Live cell imaging

Target cells were cultured on glass coverslips (25 mm or 30 mm diameter) and labeled with DiO (Invitrogen, concentration 5 μ M) to label the membrane. Calcein-AM green or -red-orange (concentration 10 μ M, Invitrogen) was used to label the cytoplasm of the target cells. In some experiments, as stated in the Figure legends, TO-PRO-3 iodide (1 μ M concentration, Invitrogen) was present in the culture medium during imaging. Target cells were incubated with PMNs in E:T ratio 5:1 for periods up to 4 hr at 37°C and 5% CO₂ in IMDM culture medium supplemented with 20% (v/v) FCS. Imaging was started within 5 min after initiation of the experiment and was performed at various indicated times and intervals either in a LSM 510 META laser scanning microscope (Carl Zeiss) microscope, or in a Leica TCM sp8 confocal microscope (Leica).

Intravital microscopy of the liver

Experimental B16F10 liver model

Lysm-egfp knockin reporter mice (Dr. T. Graf, Albert Einstein College, New York) and *Lysm-egfp/Sirp α Δcyt* mice (Inagaki et al., 2000) were used for visualization of hepatic neutrophils.

Animals were anesthetized by intraperitoneal injection of a mixture of 200 mg/kg ketamine (Bayer Animal Health) and 10 mg/kg Xylazine (Bimeda-MTC). The right jugular vein was cannulated to administer additional anesthesia and propidium iodide to visualize necrotic cells (Sigma-Aldrich). Surgical preparation of the liver and intrasplenic injection of tumor cells was done as briefly described in the following. Laparotomy along the linea alba was performed followed by removal of the skin and abdominal muscle along the costal margin to the mid axillary line to expose the liver. Melanoma (B16F10) cells (2 \times 10⁵) were labeled with fluorescent DiI or DiD membrane dye (Sigma-Aldrich) and injected into the spleen. Mice were splenectomised shortly after injection of the B16F10 cells.

Therapeutic antibody (TA99, BioXcell, 200 μ g) was injected intraperitoneal 2 h prior to intravital microscopy. To deplete Kupffer cells, mice were injected with 200 μ L clodronate liposomes (0.69 mol/L) intravenously 48 h prior to the start of the experiment. For depletion of neutrophils, mice were injected twice with anti-Ly6G antibody (clone 1A8) 72 h prior and at the start of the experiment. For blocking CD47-SIRP α interactions, B16F10 melanoma cells (1 \times 10⁶) were incubated with 10 μ g of SSL6 (kind gift from J.A. van Strijp and P.J.A. Haas) and intrasplenically injected after repeated washing.

Intravital microscopy of B16F10 liver model

Spinning-disk multichannel-fluorescence intravital microscopy of mouse liver was performed with an Olympus IX81 inverted microscope, equipped with an Olympus focus drive and a motorized stage (Applied Scientific Instrumentation, Eugene, OR, USA) and fitted with a motorized objective turret equipped with 4X/0.16 UPLANSAPO, 10X/0.40 UPLANSAPO and 20X/0.70 UPLANSAPO objective lenses and coupled to a confocal light path (WaveFx; Quorum Technologies, Guelph, ON, Canada) based on a modified Yokogawa CSU-10 head (Yokogawa Electric Corporation, Tokyo, Japan). The mice were placed on the right lateral position and the liver was exteriorized on a heated microscope stage. All exposed tissues were moistened with saline-soaked gauze to prevent dehydration during image acquisition. For all experiments body temperature was maintained and the liver continuously superfused with physiological saline buffer. Volocity software (Perkin Elmer) was used for image acquisition.

Staining of tumor samples from breast cancer patients

Breast tumor samples from a female Her2/Neu- positive patient (see Figure S5C for patient characteristics) were embedded in paraffin, cut into 4- μ m sections and further processed as previously described (Suzuki et al., 2015). Briefly, tissue sections were deparaffinized and rehydrated, and endogenous peroxidase activity was quenched with 3% hydrogen peroxide. Furthermore, sections were blocked with 5% (v/v) normal goat serum (Abcam), and incubated with anti-MPO and anti-HER2 (Ready to use, clone 4B5, rabbit monoclonal, Roche). Appropriate secondary antibodies were applied for 1 hr, after which sections were stained with MACH2 double stain 2 (Biocare Medical). In accordance with the Declaration of Helsinki, informed consent was obtained from all breast cancer patients.

QUANTIFICATION AND STATISTICAL ANALYSIS

Data analysis and statistics

Flow cytometry data were analyzed by Flowjo software (Tree Star, Inc, Ashland, OR, USA). Image analysis of the intravital B16F10 tumor model imaging was done with Volocity (Perkin Elmer) and ImageJ (NIH).

Where appropriate, figure legends define n and the dispersion and precision measures. Data are expressed as mean \pm 1 SEM, unless otherwise specified. For each experiment, unless otherwise noted, n represents the number of individual biological replicates. Statistical differences between two groups were tested in Prism (Graphpad) by t test; multiple comparisons were tested by One-way ANOVA-test followed by Sidak post hoc test for correction of multiple comparison. In the overall analysis of the LOPAC library

screening, for each compound the distribution of the experimental values for replicates, readouts and CD47 condition (wild-type versus knockdown) was compared with the distribution of the negative controls in the Wilcoxon-test. The resulting p values were corrected for multiple testing by the Benjamin Hochberg method.

DATA AND SOFTWARE AVAILABILITY

Hits found by use of the LOPAC library are presented in [Table S1](#).